STRUCTURAL AND CHEMICAL CHANGES IN THE TOPOCHEMICAL 1,4-POLYMERIZATION OF 3,4-BIS(METHYLENE)HEXANEDIOIC ACID

A thesis presented to the faculty of the Graduate School of
Western Carolina University in partial fulfillment of the
requirements for the degree of Master of Science in Chemistry.

By

Christopher Alan Steddum

Director: Dr. Brian Dinkelmeyer
Associate Professor of Chemistry
Chemistry and Physics Department

Committee Members: Dr. Scott Huffman, Chemistry
Dr. Channa De Silva, Chemistry

March 2012

ACKNOWLEDGEMENTS

In addition to the members of my thesis research advisory committee, I would like to thank the entire faculty and staff of the Chemistry and Physics department for offering advice and answering countless questions. Acknowledgement is also due to Kyle Beard and Shauna Weathersby; the members of Dr. Dinkelmeyer's research group who performed previous work to lay the ground for my research. Furthermore, thanks to Robert D. Pike of the College of William and Mary for providing crystallographic data. I am also very grateful for the friendship and support of my fellow graduate students in the Chemistry and Physics department. Without them, my time spent in Cullowhee would not have been so enjoyable.

TABLE OF CONTENTS

LIST OF TABLES

LIST OF FIGURES

ABSTRACT

STRUCTURAL AND CHEMICAL CHANGES IN THE TOPOCHEMICAL 1,4-POLYMERIZATION OF 3,4-BIS(METHYLENE)HEXANEDIOIC ACID

Christopher Alan Steddum, M.S.

Western Carolina University (March 2012)

Director: Dr. Brian Dinkelmeyer

Since the discovery of the topochemical 1,4-polymerization of 3,4-bis(methylene)hexanedioic acid (BMHA), the first reported polymerization of an internally substituted butadiene, an objective of our research group has been to characterize the chemical and structural changes undergone by the crystalline monomer during polymerization. Here, we report a method for the kinetic study of topochemical reactions. BMHA exhibits first order kinetics with a rate constant, *k*, of 0.215 min^{-1}. Compared to the polymerization of *(Z,Z)*-2,4-hexadienedioate (EMU), discovered by Matsumoto et al., which also has first order kinetics with a rate constant, *k*, of 0.394 min^{-1}, BMHA reacts slightly slower than EMU. In addition to kinetic data, structural changes in the polymerization of BMHA were assessed by X-ray powder diffraction. The reaction of BMHA is heterogeneous with polymerization beginning at defect sites in the crystal which serve to nucleate polymer growth in distinct domains that propagate through the monomer lattice. Further, differential thermal analysis demonstrates the polymerization of BMHA by heating (T_p = 165 °C). By comparing the heat of polymerization of BMHA to the heats of polymerization of liquid butadiene analogues, the energy of the lattice strain overcome during the crystal structure transformation can

be approximated at 43.3 kJ/mol. The information reported in this work serves to characterize the topochemical polymerization of 3,4-bis(methylene)hexanedioic acid.

CHAPTER ONE: INTRODUCTION

1.1 Research Objectives

Organic solid state reactions have been known for a long time but have gained attention in the last decade for their usefulness in selective organic synthesis.[1] The desire to understand structural and chemical changes in crystalline reactions leads to a new set of challenges and the need to apply novel methods for monitoring these changes. The purpose of this research study is to develop a method for measuring the rates of organic solid state photochemical reactions, to monitor the structural changes in the crystal lattice during the polymerization of 3,4-bis(methylene)hexanedioic acid (BMHA), and to determine the heat of polymerization of BMHA.

Methods for studying the rates of topochemical polymerizations have been established by Matsumoto et al. and have been successfully applied to polymerizations developed in his research group.[2] These methods are neither standardized nor well documented making them difficult to apply in other laboratories. Our goal is to create a method which will serve as a standard in our research group to allow the measurement and comparison of rates of a variety of topochemical reactions developed in house as well as reactions developed by other researchers. This will provide a tool by which to compare reaction rates for a better understanding of the parameters which control rate in the solid state.

An additional goal is to track the structural changes, or changes in the spacing of the crystal lattice, of BMHA during its polymerization. Understanding how the crystal lattice changes during reaction is an essential part of understanding the polymerization mechanism as well as the molecular movements which accompany the reaction.

A side project, and final research objective, was to determine the enthalpy change associated with the polymerization of BMHA. The enthalpy of polymerization, ΔH_p, was determined by measuring heat flow during thermal initiation of the polymerization by differential thermal analysis (DTA). Heating BMHA initiates polymerization while previously the monomer crystal was believed to melt.[3] This is not tremendously rare as many examples of topochemical reaction induced by heating have been published.[4] A crude estimate of the lattice strain energy is possible by comparing the enthalpy of polymerization of BMHA with the heats of polymerization of liquid butadiene analogues.

1.2 Topochemical Reactions

The field of topochemistry was founded by Schmidt and Cohen who proposed the topochemical postulate while studying the solid state reactivity of cinnamic acid. The topochemical postulate states that solid state reactions proceed with a minimum amount of molecular and atomic movement and with minimum distortion to the crystal lattice.[5] The postulate explains that atoms must be in close contact in order for bonds to form, or that there must be a short, defined distance between atoms which will form bonds. This is a direct result of the close packing of molecules within crystals which prevents large molecular movements. Bonds will form between atoms that are in Van der Waals contact or close to it.

Schmidt et al. observed that crystallographic symmetry is retained during topochemical reactions. Symmetry elements relating molecules in the reactant crystal are preserved or transferred to the products that form in these systems.[5] In their seminal work on cinnamic acids they found that polymorphic crystals, seen in Figure 1, produced different products that depended upon the molecular packing within the crystal. In one

polymorph, molecules were related by a mirror plane and the product formed by their [2+2] cycloaddition also possessed this symmetry element. A second polymorph had cinnamic acids arranged around an inversion center. The products formed similarly contained this symmetry operation.

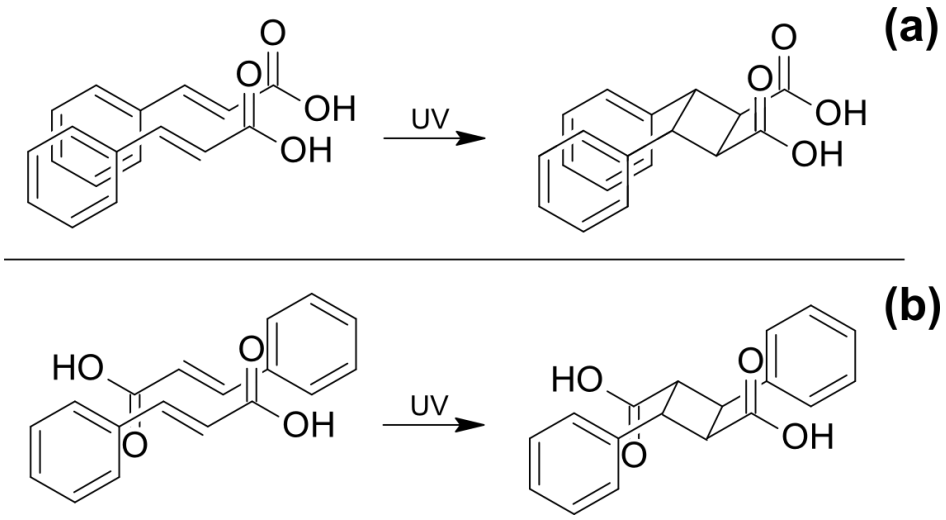

Figure 1. (a) And (b) are distinct polymorphs of cinnamic acid. The symmetry operations relating reactant molecules are retained in the products.

These same observations have been found to hold for other reactions that take place within crystals, including polymerizations. In polymerization reactions, symmetry is also retained between monomer and polymer crystals so that the space groups of both are the same.[6,7] Reactions that meet these requirements are said to be under topochemical control.

The rigidity of the crystal structure gives rise to the second part of the postulate stating that minimum distortion to the crystal lattice is necessary for reaction. This deals with the parameter of lattice strain which will be addressed often in the following results and discussion. Lattice strain is the hindrance to movement imposed upon a reactant molecule by the structure of the crystal lattice itself. Reorganization of neighboring molecules in the lattice requires energy which is called lattice strain energy. The inability

of a molecule or atom to move into the correct position for product bond formation can preclude reaction, which is why topochemical reactions are found where lattice strain, or as Schmidt put it, lattice distortion, is minimized. Lattice strain is often the largest barrier to reaction in these systems.

The inability for reaction to proceed because of lattice strain can be circumvented by defects in the crystal lattice. Defect sites are places where movement of a molecule is greater than normal due to imperfections in the packing of monomer molecules. These sites are also called reaction cavities. The extra movement allowed by the reaction cavity permits the movement necessary for product formation. In a topochemical polymerization, the reaction cavity propagates with the polymer chain so that the conversion of monomer to polymer continues.

The focus of this research study is a select group of topochemical reactions called 1,4-polymerizations.

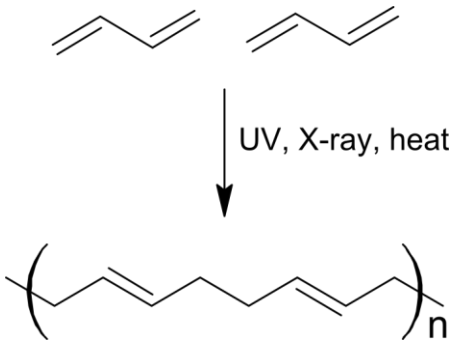

Figure 2. A generic 1,4-polymerization of a butadiene.

These are characteristic of butadienes where the 1st carbon of one diene forms a bond with the 4th carbon of the neighboring diene, shown in Figure 2. This type of addition creates polymers as opposed to dimmers seen in other topochemical additions.

Specifically, this research study investigates two topochemical 1,4-polymerizations: the polymerization of *(Z,Z)*-2,4-hexadienedioate (EMU) discovered by Matsumoto et al.[8] and the polymerization of BMHA discovered by Beard et al.[3] seen in Figure 3.

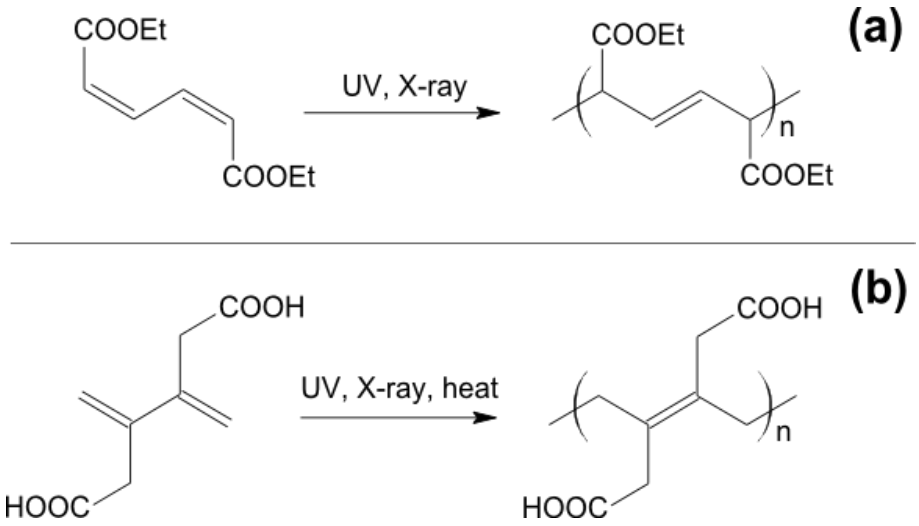

Figure 3. (a) The reaction scheme of EMU and (b) the reaction scheme of BMHA.

Matsumoto studied a number of diene esters and their solid state reactivity. They discovered that crystalline samples of those compounds underwent *cis-trans* isomerization, [2+2] cycloaddition, or 1,4-polymerization depending on the molecular packing within the crystals. They were able to determine the optimal arrangement of diene molecules after studying a small number of crystal structures for compounds that underwent the topochemical polymerization. They found that for optimal reactivity, the distance between equivalent atoms, d_s, should be ~5 Å, the distance between reacting atoms, d_{cc}, should be 4.19-4.24 Å, and the planes which define the C=C—C=C system should be offset by θ_1 ~62-67° and θ_2 ~52-55°. This arrangement, seen in Figure 4, ensures that reacting atoms are in close proximity to each other and the polymer product

can fit within the crystal lattice. It should be noted that the monomer arrangement in the BMHA system, recorded in Table 1, adheres to these parameters.

The 1,4-polymerization of BMHA was demonstrated to be topochemical in nature because both the monomer and polymer are in the $P2_1/c$ space group.[3] Crystal structures of the monomer and polymer can be seen in Figures 5 and 6, respectively. Table 1 shows the lattice spacing of the monomer and polymer.

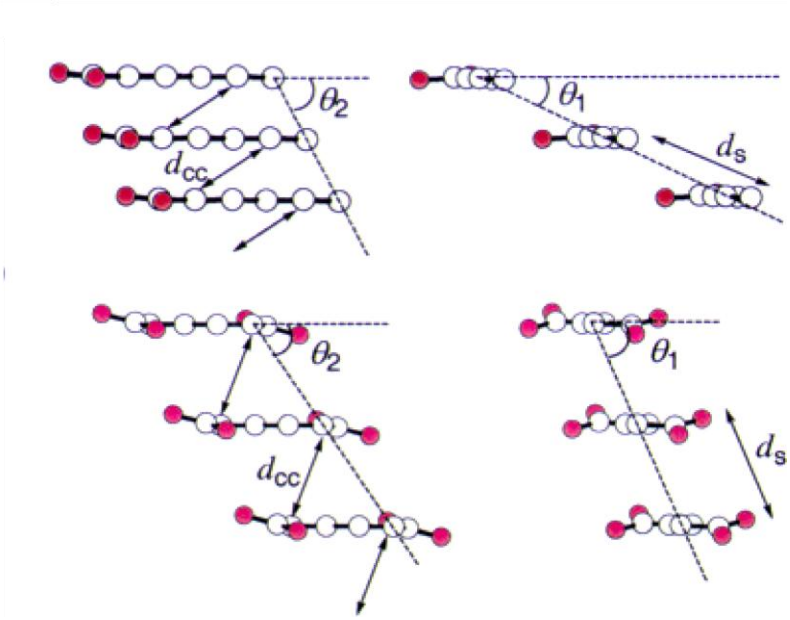

Figure 4. Structural parameters necessary for 1,4-polymerization. d_s: monomer spacing between equivalent atoms, d_{cc}: close contact distance between reacting atoms, θ_1: offset angle between plane defined by C=C—C=C, θ_2: offset angle perpendicular to θ_1.[9]

Table 1. Crystal lattice spacing for BMHA and poly-BMHA.

BMHA unit cell d-spacing (Å)	*poly-BMHA unit cell d-spacing (Å)*
a = 4.783	a = 4.803
b = 9.729	b = 8.897
c = 8.918	c = 9.016
d_s = 4.748	
d_{cc} =3.857	
θ_1 = 66.7°	
θ_2 = 52.6°	

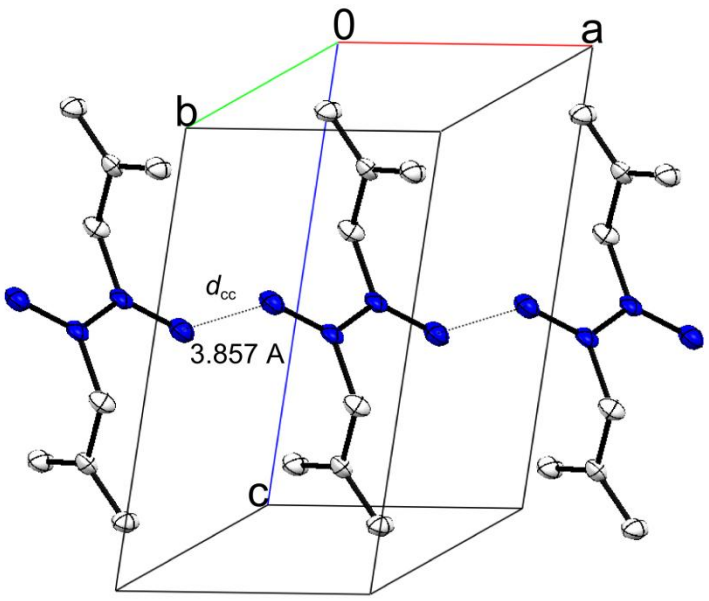

Figure 5. Crystal structure for the BMHA monomer. (Hydrogens removed for clarity; dashed lines show bonds which will form to create the polymer.)

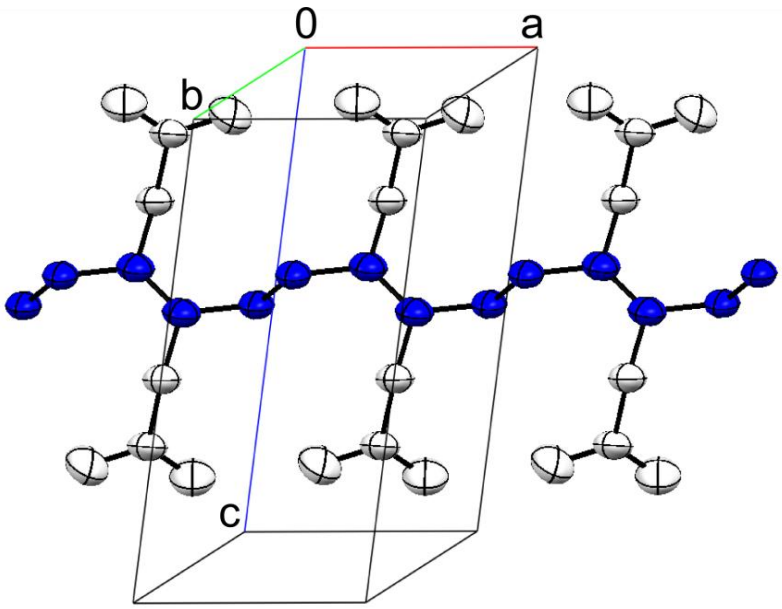

Figure 6. Crystal structure for the BMHA polymer. (Hydrogens removed for clarity.)

1.3 Kinetic Methods for Topochemical Reactions

A broad overview of chemical kinetics is presented in the online text, Analytical Chemistry 2.0, and much of the following discussion of kinetics draws from that text.[10] Traditional kinetic theories apply to reactions taking place in solution and are based upon

the collision model where the rate of reaction is proportional to the frequency of reactant collisions and the number of collisions in which molecules are oriented properly to form product. The factors which affect reaction rates in solution are the concentration of the reactants as well as the concentration of the catalyst, if any, and the temperature of the reactants. Both of these factors affect the frequency of collisions and must be controlled in a kinetic experiment.

The kinetic study of photochemical processes is complicated by additional variables such as excitation wavelength, intensity, singlet to triplet conversion, quantum yield, and the presence of sensitizers to name a few. It might be expected that the formulation of kinetic theories for describing topochemical photochemistry would be even more complicated and elaborate. However, it is common in this field to calculate rate constants and reaction orders based on the mathematical formulations derived from collision theory. The reason for applying this vast simplification is that the slow step in light induced topochemical reactions is actually the reorganization of the molecules within the crystal as reactant crystal is transformed to the product crystal. As a result, solid state reactions are typically much slower than their solution phase counterparts and the steps preceding the slow step have no effect on the overall rate expression.

The concentration of monomer crystal affects the rate of polymerization and was kept constant at an initial concentration of 100% or one mole fraction for every kinetic measurement. Mole fraction is the common unit of concentration in crystal reactions because it gives a better description of a neat solid system. The initial infrared spectrum of the monomer crystal showed only monomer absorbance bands indicating the initial crystal was pure monomer.

Temperature is a factor in solid state reactions because it affects the order within the crystal and affects the movement of the reactant molecules.[1] Increasing temperature can foster reaction and increase the rate by allowing greater molecular movement. It can also deter reaction by causing the crystal lattice to morph into a phase in which reactants are not in proper alignment for reaction. Temperature was kept constant for each kinetic measurement performed in this study.

The wavelength and intensity of irradiating light are also important parameters in photochemical kinetic experiments. Greater light intensity leads to faster reactions since photons are a reactant in photochemical reactions. The wavelength of light is important since it must be absorbed by the reactant yet not absorbed by the product if high yields are to be achieved.[11] If the absorption spectrum of the reactant and product overlap, the wavelength at the tail end of the monomer's absorbance should be used for irradiation so that it is not absorbed by the product and light can reach reactant molecules at the interior of the crystal to induce reaction. Figure 7 illustrates this principle. The source used in our experiment is polychromatic so the problem of overlapping polymer and monomer absorption will be eliminated.

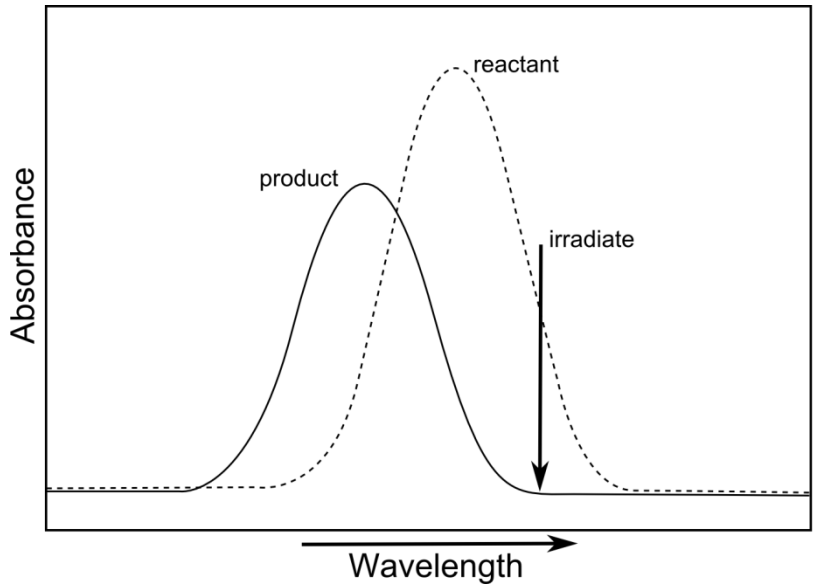

Figure 7. If reactant and product absorption spectra overlap, a wavelength which the reactant, but not the product, absorbs should be chosen for irradiation to give maximum yield.

For any kinetic experiment, measuring the rate of a reaction requires the ability to measure the concentration of the reactant and/or the product as a function of time. Fourier transform infrared spectroscopy (FT-IR) is a powerful tool for kinetic experiments in solid state reactions. Because BMHA and poly-BMHA have unique infrared absorbances, the concentration of the monomer and polymer can be determined at any point during the reaction by relating the absorbance of monomer or polymer to concentration through the Lambert-Beer law. The Lambert-Beer law, $A = \varepsilon bc$, states that absorbance is proportional to the absorptivity, ε, the concentration of the sample, c, and the path length of the sample, b. Because BMHA is a solid state reaction, mole fraction, X, is a more appropriate term than concentration, c, and will be substituted for c in the kinetic discussion. The mole fraction of the BMHA monomer with respect to time gives the rate of polymerization.

To determine the polymerization's order, a curve fitting method will be used. This requires creating plots of monomer mole fraction, X_1, the natural logarithm of mole

fraction, Ln(X_1), and the inverse of mole fraction, $1/X_1$, against time to determine if the polymerization is zero, first, or second order, respectively. The plot, if any, which reveals a linear relationship will determine the order of the BMHA polymerization.

The polymerization of EMU is known to be approximately first order, and owing to the similarity between the polymerization of EMU and BMHA, BMHA will likely exhibit a first order reaction rate.[12] The mechanism for the polymerization of BMHA can be approximated as a unimolecular, non-reversible reaction with the reaction equation

$$\text{BMHA} \xrightarrow{k} \text{poly-BMHA}$$

In addition to measuring the rate and determining the rate law and rate constant for BMHA, the same will be done for EMU. The method employed to gather kinetic data will be a relative method so that reactions performed by this method will be comparable, but they will not be comparable to reaction rates determined in other laboratories with different methods such as those used by Matsumoto. Determining the rate of polymerization of EMU with our method will serve as method verification as well as allow direct comparison of the rate of EMU to that of BMHA.

1.4 Monitoring Structural Changes by X-ray Powder Diffraction

In addition to FT-IR kinetic data, which provides information on chemical changes, it is useful to know how the crystal lattice is changing during the course of polymerization. X-ray powder diffraction (XRD) is a good tool for monitoring these changes. Changes in the diffraction pattern during reaction provide information on how the crystal lattice adjusts as it is transformed into the product crystal. From these changes it is possible to infer the molecular movements during reaction, such as an unpacking event, information about the loss or retention of crystallinity in the polymer, and whether

the reaction is a homogeneous or heterogeneous process. Because the polymerization of BMHA proceeds under X-ray irradiation, the changes in the crystal structure during polymerization can be monitored by continuous X-ray diffraction measurement until polymerization is complete. Infrared analysis can confirm that poly-BMHA is formed by X-ray irradiation.

In a homogeneous reaction, reaction is initiated randomly throughout the crystal. During intermediary stages, the crystal appears as a solid crystalline solution containing both reactant and product. A homogeneous reaction is possible if there is little lattice strain and the crystal structure of the reactant and product phases are very similar.

In a heterogeneous reaction, crystalline domains containing product act as nucleation sites for the transformation of reactants to products. It is thought that the boundary of the product phase provides a surface that helps organize reactants for reaction. Under these conditions lattice mismatches between reactant and product phases may cause cracking and disorder in the crystal. A large mismatch between reactant and product lattices can result in destruction of the crystal, cessation of the reaction, or the introduction of disorder with the loss of topochemical control. Heterogeneous reactions often start at the surface or at defect sites and then propagate through the crystal. The product phase continues to grow through the crystal until the reaction is complete. Schematics of a heterogeneous and a homogeneous topochemical polymerization can be seen in Figure 8.

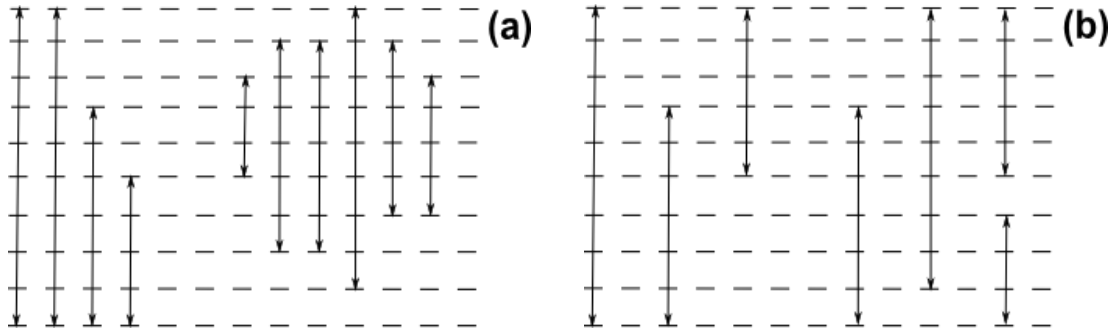

Figure 8. (a) Heterogeneous polymerization showing polymer propagation from defect sites and (b) homogeneous polymerization with polymer chains growing at random.

Topochemical polymerizations typically exhibit one of the following three behaviors which are evidenced by XRD analysis. The first and ideal situation results in a smooth and continuous homogeneous crystal-to-crystal transformation to give product in high yield where the products formed retain crystallographic symmetry. A less optimal outcome occurs when reactant crystals undergo a heterogeneous process and are transformed to products with some cracking and introduction of disorder to the crystal. Lastly, a partial transformation of products in either low yield and/or with the loss of topochemical control with destruction of the crystal lattice occurs. These different modes of behavior can be observed by analyzing the changes in the XRD patterns during the polymerization.

In the first scenario, the reaction occurs uniformly and homogeneously throughout the crystal with little lattice strain. In this case, peaks in the XRD spectrum will broaden and shift continuously to new positions as the reaction proceeds. The broadening of peaks results from an unpacking event where reacting molecules, undergoing changes in molecular geometry, create areas of local disorder. The peaks eventually become sharper as molecules realign with the growing product crystal structure.

Alternatively, the reaction may occur heterogeneously within localized areas of the crystal typically starting on the crystal surface. This results in crystalline domains of product that grow through the crystal. In this case the sample will contain crystalline domains of both monomer and polymer. The XRD patterns during polymerization will be a combination of both the monomer and polymer crystal. This is often the case for topochemical reactions with moderate lattice strain.

Finally, the polymerization may only proceed in low yield and with loss of crystallinity. Sometimes product mixtures result due to loss of topochemical control. In this case *all* of the peaks in the XRD pattern become broadened and eventually disappear as the crystal becomes amorphous. This behavior is typical of reactions with high lattice strain.

1.5 Enthalpy Changes Observed by Differential Thermal Analysis

Differential thermal analysis (DTA) will be performed to heat BMHA steadily to look for evidence of polymerization. Tracing heat flow as a function of temperature shows endotherms or exotherms as a result of physical or chemical changes such as a melt or a reaction. Polymerizations, in general, are exothermic so evidence of an exotherm may suggest polymerization of BMHA by heat. Infrared analysis can be used to confirm the polymerization. These experiments will also provide data on the thermodynamic changes associated with the heat induced polymerization of BMHA.

With evidence of thermally initiated polymerization from DTA, it is possible to calculate the energy exhumed per mole of BMHA. If the enthalpy of the chemical changes and the enthalpy of lattice strain are the major contributors to the enthalpy of the polymerization, it is possible to calculate a crude estimate of the lattice strain energy.

Lattice strain in topochemical reactions refers to the energetic barrier that must be overcome for the small molecular movements necessary for reaction. This barrier arises from the crystalline environment around reactant molecules which restricts movements which are necessary for a reaction to take place. Reactions that require large amplitude movements of reactant molecules have larger lattice energies than reactions that require little atomic movement.[11]

The lattice strain can be calculated by proposing that the enthalpy of polymerization of BMHA is the sum of the energy given off by the chemical change (bond breakage and formation) and the energy of the lattice strain which must be overcome in order for the monomer molecules to move into proper alignment for polymer formation. Using literature values for the heat of polymerization of liquid butadiene (CH_2=CH—CH=CH_2) as an estimation of the energy of chemical change during the topochemical polymerization of BMHA allows a crude calculation of the lattice strain energy since the total enthalpy of polymerization is known from DTA.

CHAPTER TWO: RESULTS AND DISCUSSION

2.1 Differential Thermal Analysis

Controlled heating of BMHA by differential thermal analysis reveals that the polymerization proceeds under heating, and that the process is not reversed when poly-BMHA is cooled. The initiation of the polymerization occurs at 165 °C. Table 2 displays the results of the three DTA measurements of the BMHA polymerization. Upon visual inspection, poly-BMHA appeared as an off-white crystalline powder after undergoing thermal polymerization, which is identical to the appearance of poly-BMHA crystals after polymerization by ultraviolet irradiation.

Infrared analysis provides further evidence that the exotherm recorded by DTA, shown in Figure 9 was the reaction to yield poly-BMHA. Figure 10 shows the known poly-BMHA infrared spectrum with the infrared spectrum of the polymer formed by heating for comparison. The spectra are nearly identical, demonstrating the thermally initiated polymerization of BMHA. Thermal initiation of EMU was not possible since the monomer crystal melts between 53-54 °C.[8]

Table 2. DTA polymerization results for BMHA for three redundant trials.

DTA trial	*Exotherm temperature (°C)*	*Temperature of peak heat flow (°C)*	*ΔH_p (kJ/mol)*
1	165-183	176.76	-29.3512
2	165-182	176.59	-28.9560
3	164-182	177.45	-30.0446
Average ±Std. Dev.		176.9±0.4	-29.5±0.5

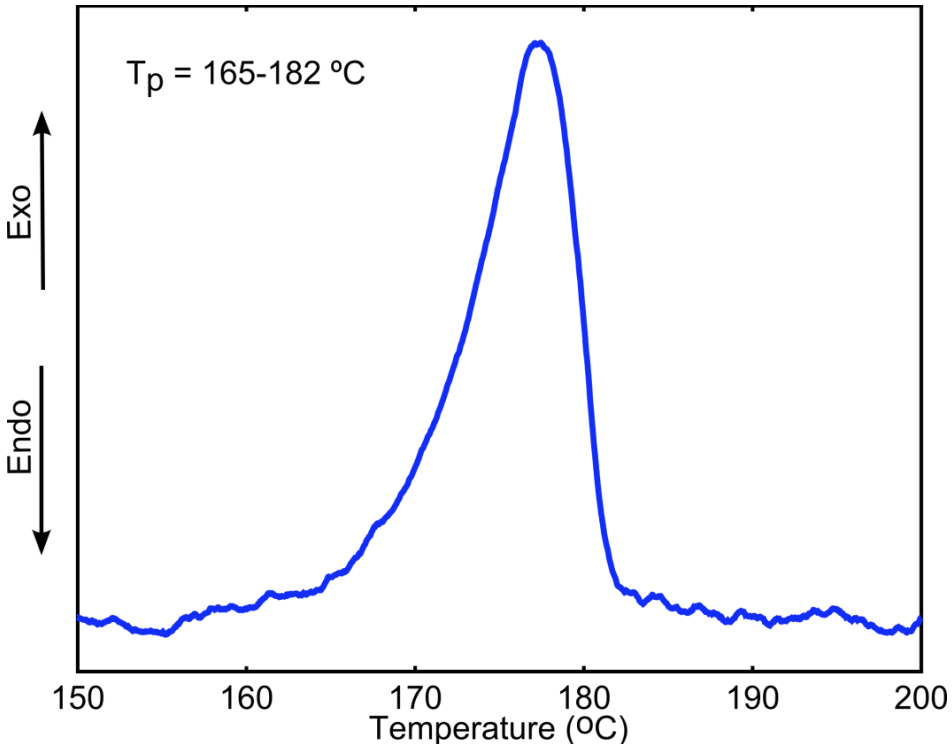

Figure 9. DTA trace of heat flow during the polymerization of BMHA showing an exotherm from 165-182°C.

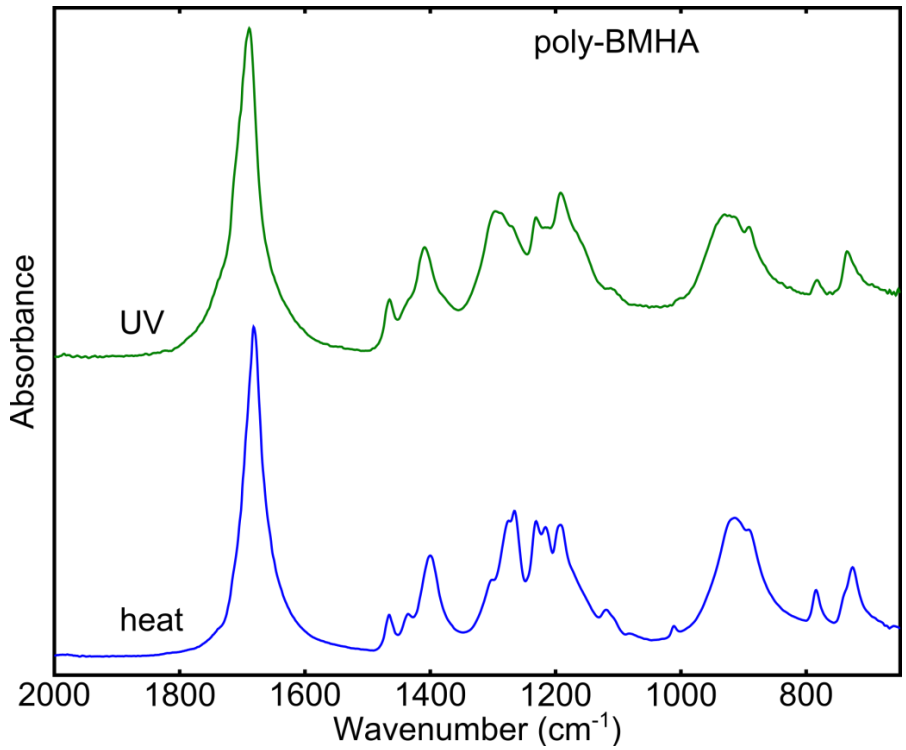

Figure 10. Infrared spectrum of poly-BMHA formed by UV irradiation compared to the spectrum of poly-BMHA which resulted from heating during DTA measurement.

When the heat of polymerization of BMHA is compared to literature values for the heats of radical initiated polymerizations of similar butadienes in the bulk liquid phase, BMHA exhibits a significantly lower quantity of heat released per mole. Summarized in Table 3, these values indicate that some endothermic process must be taking place during the topochemical polymerization of BMHA. The reason the BMHA polymerization liberates less energy per mole than the bulk polymerization of liquid butadiene is that the BMHA polymerization requires the reorganization of the monomer crystal lattice to that of the polymer product lattice during the transformation. This lattice reorganization is an endothermic process which decreases the exotherm of the overall reaction.

Table 3. Heats of polymerization for BMHA compared to solution butadiene radical addition polymerizations.[13,14]

Butadiene monomer	*Structure*	*$-\Delta H_p$ (kJ/mol)*	*$-\Delta H_p$ (kcal/mol)*
BMHA (crystal)		29.5	7.0
Butadiene (liquid)	CH_2=CH—CH=CH_2	72.8	17.4
Isoprene (liquid)	CH_2=C(CH_3)—CH=CH_2	74.5	17.8

Additionally, we propose that the enthalpy of polymerization of BMHA is the sum of the enthalpy of the chemical change (bond breakage and formation) and the enthalpy of the lattice strain associated with the crystal lattice rearrangement. The enthalpy change due to chemical change in the BMHA polymerization should be similar to the enthalpy change of liquid butadiene polymerization since the same bonds are broken and formed in both the BMHA solid state polymerization and the butadiene liquid state polymerization. The difference between the enthalpy of polymerization of BMHA and the enthalpy of polymerization of liquid butadiene should approximate the enthalpy difference of the reactant and product crystal lattice. The equation showing the proposed breakdown for the heat of polymerization of BMHA can be written

$$\Delta H_{rxn} = \Delta H_p + \Delta H_{st}$$

Where ΔH_{rxn} is the enthalpy of the topochemical polymerization of BMHA, ΔH_p is the enthalpy of the chemical change of the BMHA polymerization, and ΔH_{st} is the energy of the lattice strain, graphically represented in Figure 11.

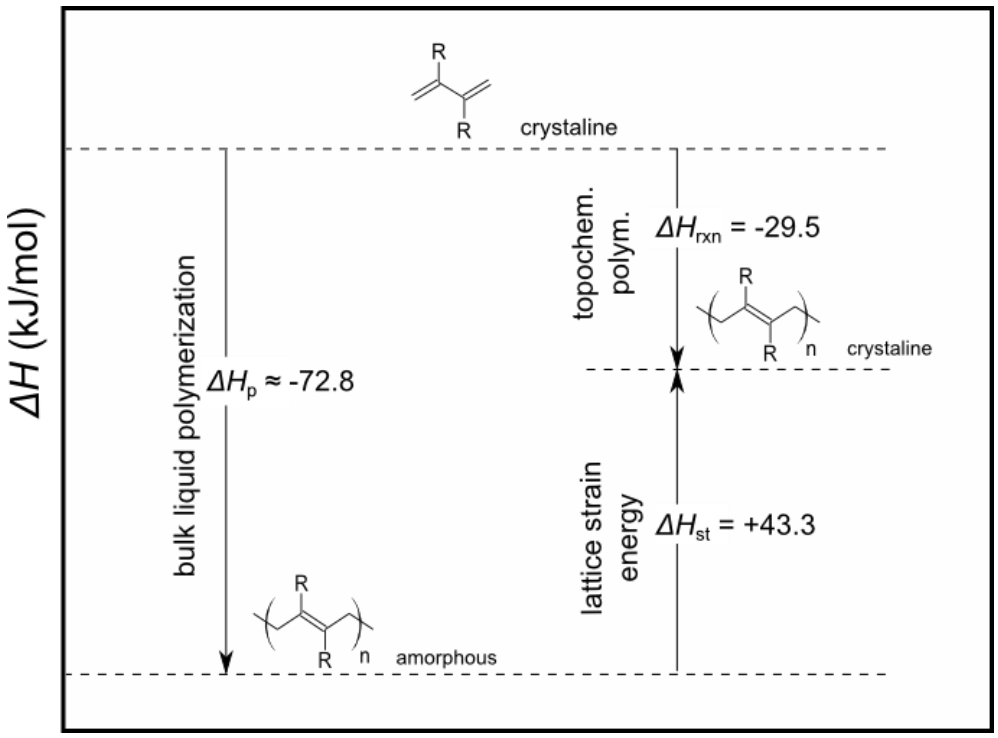

Figure 11. Born-Haber diagram for proposed calculation of lattice strain energy in the topochemical polymerization of BMHA.

If the energy evolved from the chemical change of the polymerization is proposed to be equal in magnitude to the heat of the liquid polymerization of butadiene, then the lattice strain energy may be calculated by rearranging the above equation for the heat of polymerization and solving for ΔH_{st}.

$$\Delta H_{st} = \Delta H_{rxn} - \Delta H_p$$

$$\Delta H_{st} = -29.5\, kJ/mol - (-72.8\ kJ/mol)$$

$$\Delta H_{st} = 43.3\, kJ/mol$$

Therefore, the energy of the lattice strain for the polymerization of BMHA can be approximated at 43.3 kJ/mol. This is only an approximation based on the proposal outlined above.

2.2 X-ray Powder Diffraction

When comparing the BMHA monomer and polymer X-ray diffraction patterns shown in Figure 12, many sharp X-ray reflections are seen in the monomer diffraction pattern, while significantly fewer reflections and broader peaks are observed in the polymer diffraction pattern. In fact, the predicted pattern for the polymer, calculated from single crystal diffraction data, resembles the monomer pattern with adjustments in the placement of the reflection peaks. Despite the differences between the calculated and measured powder patterns for poly-BMHA, infrared analysis confirms polymer synthesis.

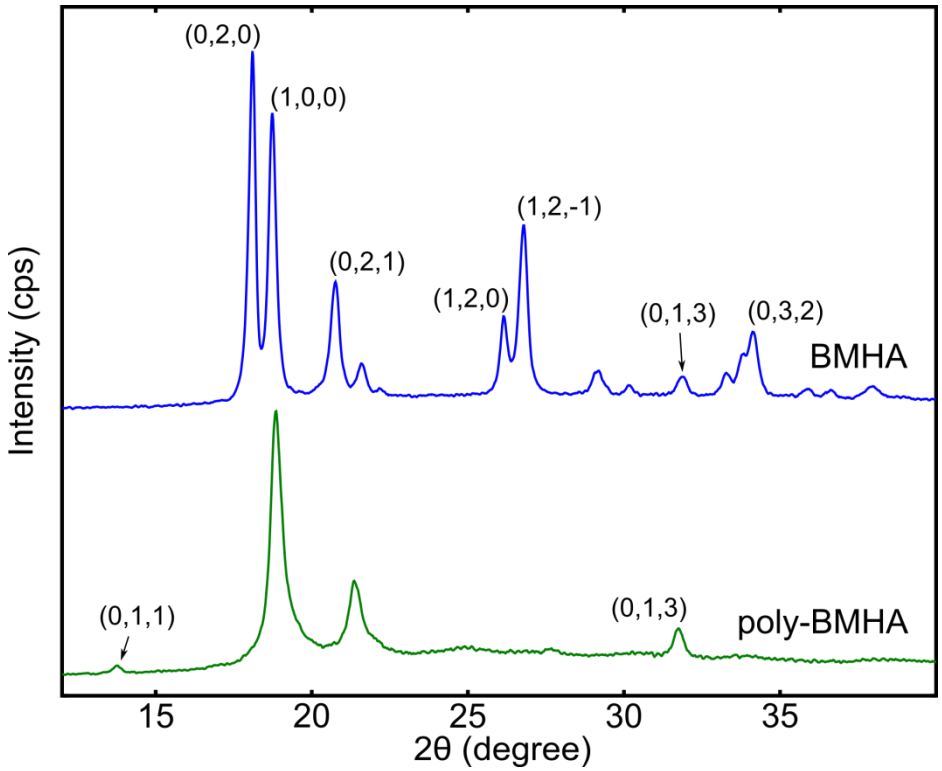

Figure 12. X-ray powder diffraction patterns for BMHA monomer and polymer with selected h,k,l planes labeled.

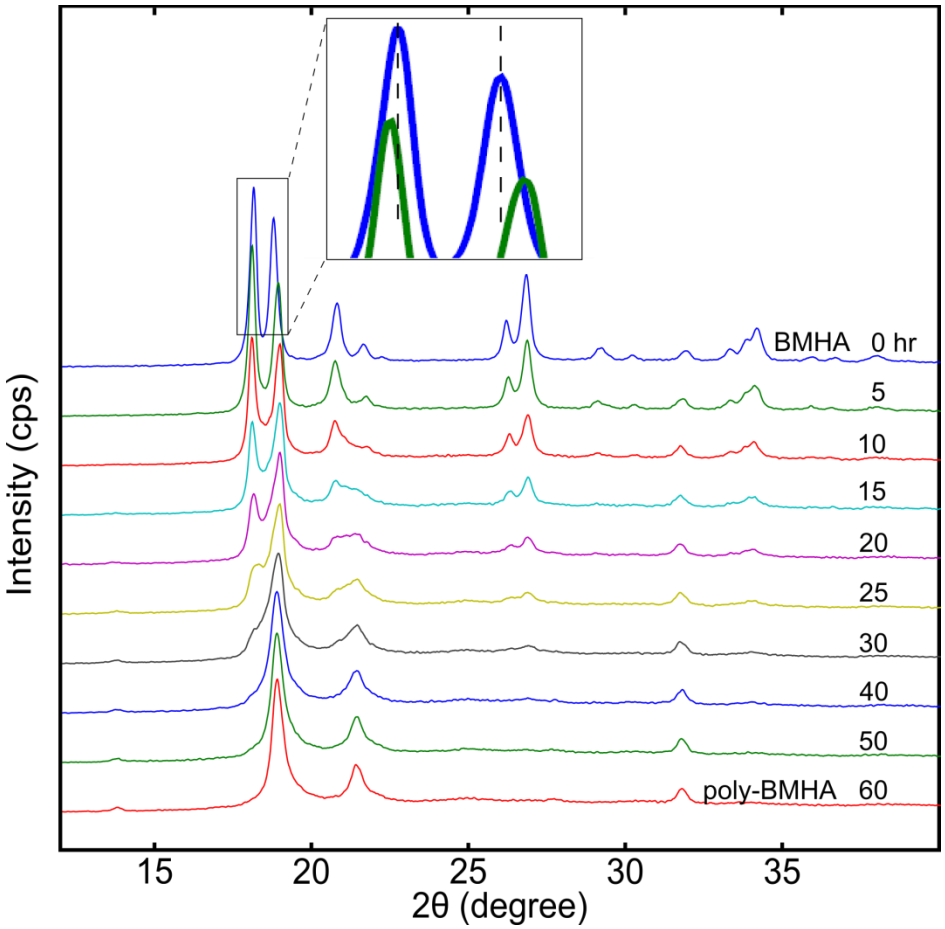

Figure 13. Changes in the X-ray diffraction patterns as BMHA polymerizes.

The absence of predicted peaks in the measured polymer diffraction pattern is an indication of the loss of some degree of crystallinity when the polymer if formed. Looking at the diffraction patterns over the course of the polymerization, as shown in Figure 13, there is a gradual disappearance of peaks representing the monomer rather than a continuous lateral shift of peaks to give the polymer diffraction pattern. These gradual losses of reflection intensity are best illustrated by the signals around 18, 27, and 34 degrees. The growth of a reflection unique to the polymer appears around 14 degrees. This behavior is indicative of a heterogeneous topochemical reaction in which the polymerization begins at defect sites which serve as a nucleus for polymer propagation.[11]

Additionally, the time lapse X-ray diffraction patterns show an unpacking event which precedes polymerization. At five hours, before significant conversion of monomer to polymer has taken place, the two tallest reflections around 18 and 19 degrees have shifted to lower and higher angles, respectively, shown in Figure 13 (inset), which demonstrates shifting in the planes of the crystal lattice. This shifting in the lattice is likely the molecular movement required for the first domains of polymer to form and begin propagating throughout the crystal lattice.

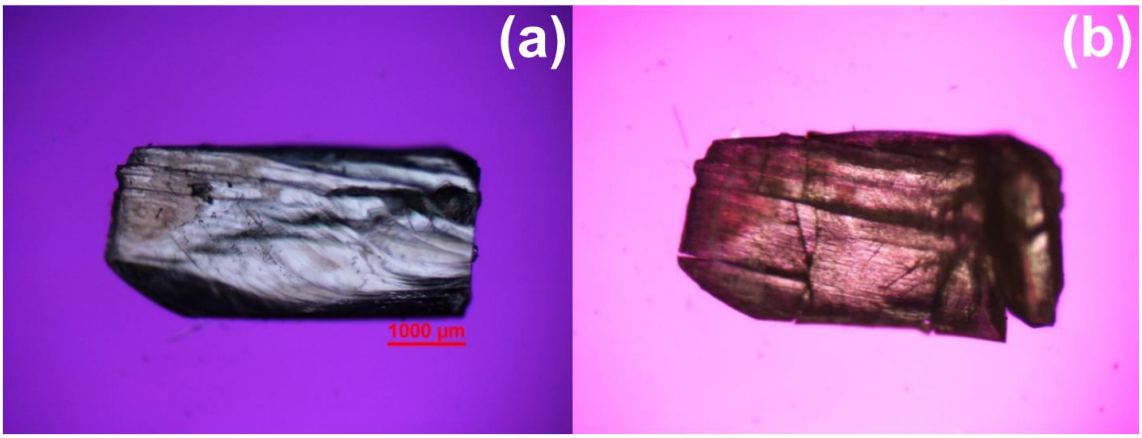

Figure 14. (a) BMHA crystal and (b) the same crystal irradiated for 112 minutes by high-pressure mercury vapor lamp. Crystal fracturing is evident due to lattice strain associated with polymer formation.

Changes in the X-ray diffraction patterns over the course of the polymerization indicate that the reaction of BMHA exhibits a heterogeneous lattice reorganization mechanism. A heterogeneous polymerization is defined by polymer formation in many domains in the monomer lattice, followed by propagation of the polymer from those domains until the crystal lattice is completely polymer. Heterogeneous reactions involve lattice strain in the crystal transformation, reported by Wegner et al.,[11] which is evidenced in the polymerization of BMHA by reduction in crystallinity of poly-BMHA, shown in XRD analysis, and evidenced further by fracturing of the polymer crystal during bulk

polymerization of BMHA. Figure 14 shows cracking and fracturing of BMHA as the polymer forms under irradiation of a high-pressure mercury vapor lamp.

2.3 FT-IR Kinetic Study

For the polymerization of BMHA, the relative concentrations of monomer and polymer can be measured by monitoring the changes in absorbance at 1605 cm^{-1} and 1466 cm^{-1}, respectively, as determined in the literature.[3] These absorbance bands are the molecular vibrational modes unique to the BMHA monomer and polymer shown in Figure 15. The infrared spectrum of both the monomer and polymer can be seen in Figure 16 showing well resolved monomer and polymer absorbance bands making relative concentration determination possible. Shown in Figure 17a, the decreasing concentration of the monomer is proportional to the disappearance of the conjugated diene stretch at 1605 cm^{-1}. The growth of the methylene -CH_2- peak at 1466 cm^{-1}, seen in Figure 17b, is proportional to the concentration of the polymer.

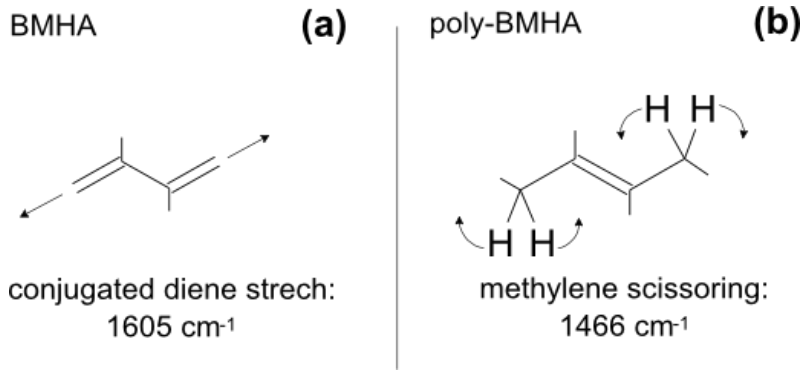

Figure 15. (a) Partial structure of BMHA showing the conjugated diene stretch IR absorbance at 1605 cm^{-1} and (b) the poly-BMHA methylene (-CH_2-) scissoring IR absorbance at 1466 cm^{-1}.

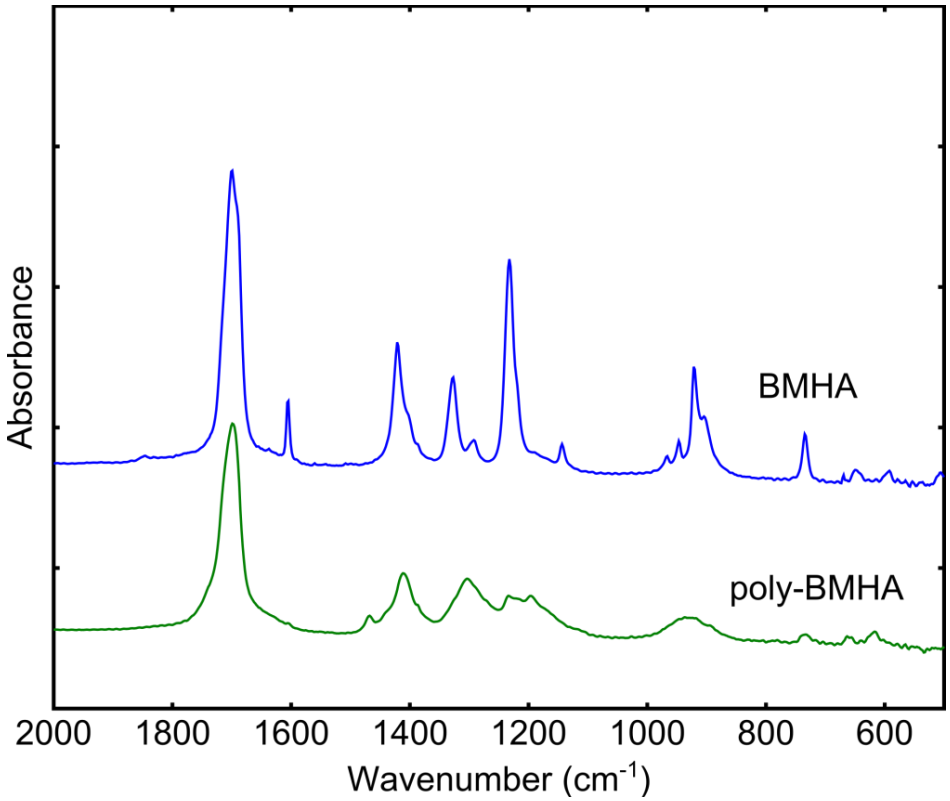

Figure 16. Infrared spectrum of BMHA monomer compared to the polymer. The spectral changes allow the determination of the monomer and polymer concentration as a function of time.

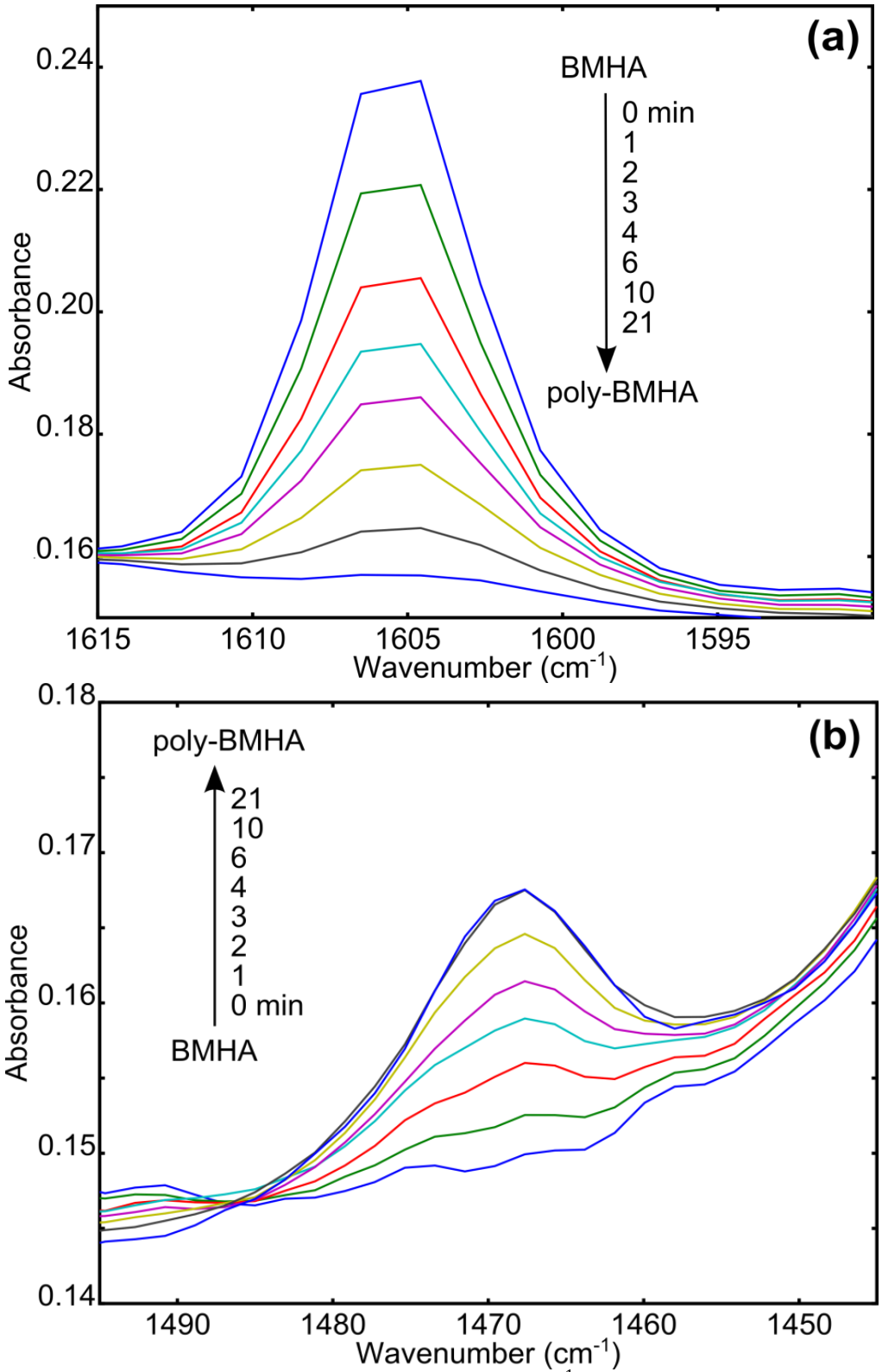

Figure 17. (a) The BMHA absorbance at 1605 cm^{-1} disappears gradually as the polymerization proceeds and (b) the poly-BMHA absorbance at 1466 cm^{-1} grows in as the polymer is formed.

Figure 18 displays a plot of the baseline subtracted absorbance values at 1466 and 1605 cm^{-1} vs. UV irradiation time for the BMHA polymerization. Baseline subtraction was necessary for our treatment of the data so that the absorbance of only the monomer and polymer were measured and not the absorbance or scattering of light from the KBr matrix. Since the baseline was stable over the course of the polymerization, baseline subtraction is consistent. At 1466 cm^{-1}, where the polymer peak grew in, the absorbance at time zero was subtracted from all subsequent spectra so that at time zero the absorbance was zero and therefore the concentration of polymer was also zero. At 1605 cm^{-1} where the monomer peak disappeared, the absorbance of the final spectrum (when monomer mole fraction was approximately zero) was subtracted from all previous spectra so that the concentration of monomer was zero at the end of the polymerization. The concentration of the monomer was not, in fact, zero at the end of the polymerization because a minute peak is visible at 1605 cm^{-1} when the reaction is complete. To avoid estimating the absorbance at which monomer concentration was zero, the absorbance value at 1605 cm^{-1} of the final spectra was used as the baseline, and subtracted from the previous spectra. This simplification is reasonable because the polymerization was estimated to achieve near completion, so the absorbance used to approximate zero monomer was nearly the same as the actual absorbance of zero monomer. The same baseline subtraction technique was performed on infrared spectra for the kinetic study of EMU, except at 1591 and 986 cm^{-1} instead of at 1605 and 1466 cm^{-1} for monomer and polymer absorbance, respectively.

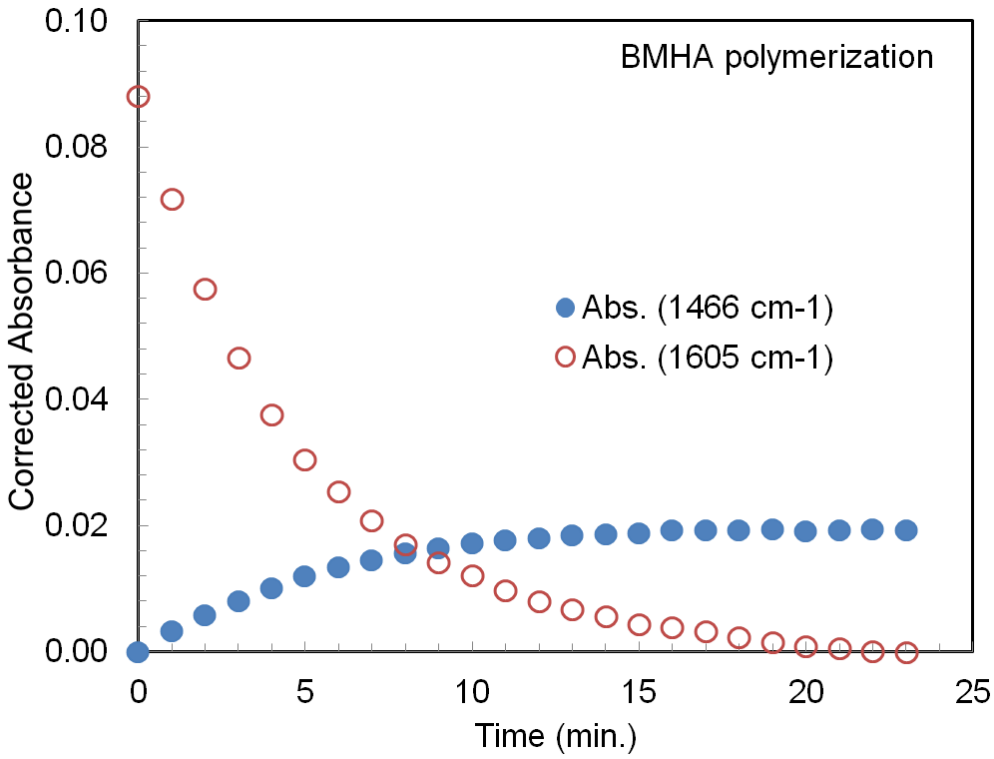

Figure 18. BMHA monomer corrected absorbance (1605 cm^{-1}) and poly-BMHA corrected absorbance (1466 cm^{-1}) as a function of UV irradiation time. On average, the reaction was complete in 22 minutes.

The *(Z,Z)*-diene, EMU, is known to polymerize by UV irradiation obeying a pseudo first order rate law. Pseudo first order rate laws are common for solid state reactions, whose slow step involves a structural change of the crystal lattice, while the fast step is the formation of polymer bonds. The data reported for EMU and the processing technique for monomer mole fraction determination over time are reported in the literature.[2] The EMU study was repeated for method verification and to be able to compare the rate of BMHA with EMU.

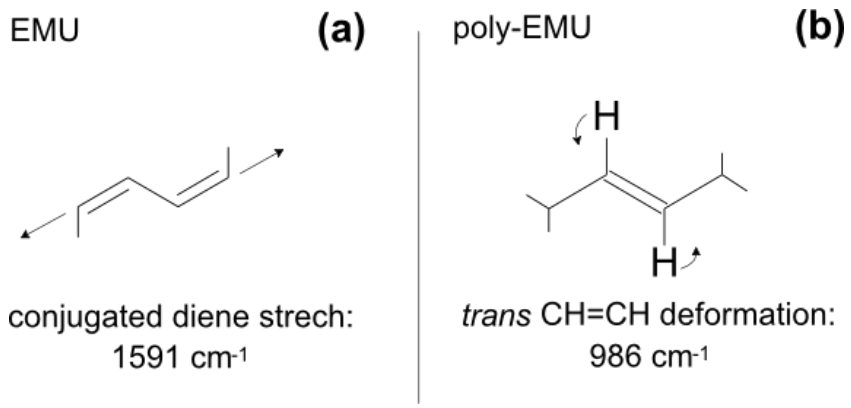

Figure 19. (a) Partial EMU structure showing the conjugated diene stretch IR absorbance at 1591 cm^{-1} and (b) poly-EMU *trans* CH=CH out-of-plane deformation IR absorbance band at 986 cm^{-1}.

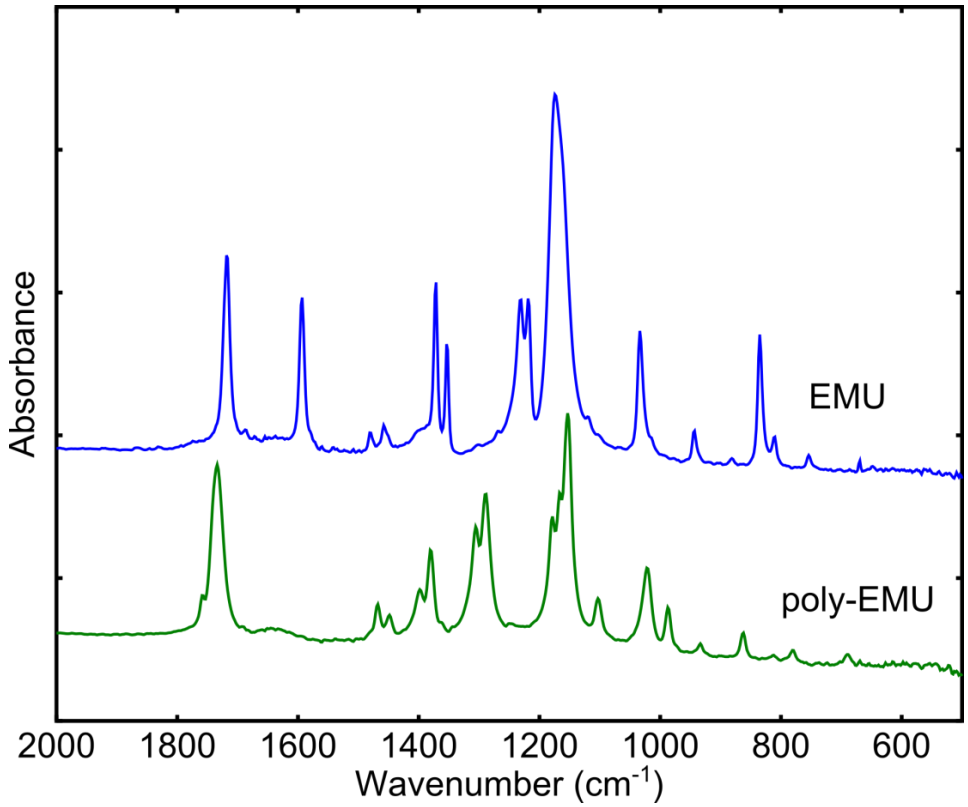

Figure 20. Infrared spectrum of EMU monomer and EMU polymer. The spectral changes allow the determination of monomer concentration as a function of time.

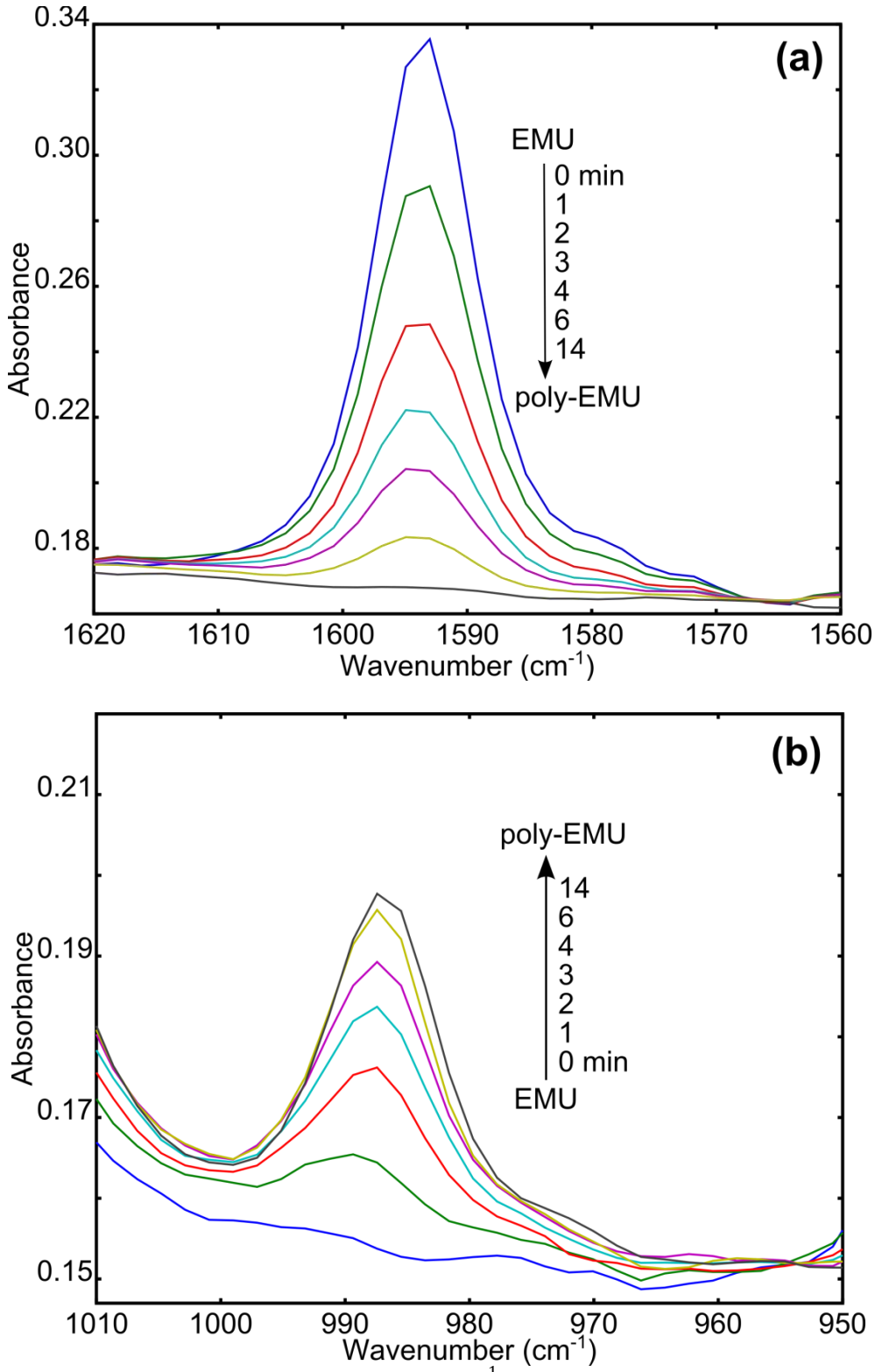

Figure 21. (a) The EMU absorbance at 1591 cm^{-1} disappears as polymerization proceeds and (b) the poly-EMU absorbance at 986 cm^{-1} appears with polymer formation.

The infrared spectrum of EMU and poly-EMU are displayed in Figure 20. During the polymerization of EMU, two important changes in the infrared spectra allow the determination of monomer and polymer concentration. Identified in the literature, absorbance bands at 1591 and 986 cm^{-1} are used to determine the concentration of monomer and polymer, respectively, as a function of UV irradiation time.[15] The absorbance band at 1591 cm^{-1} is the vibrational mode of the conjugated diene stretch of the monomer, shown in Figure 19a. The conjugated diene structure only appears in the monomer, thus is a good choice for monitoring its concentration. The absorbance band at 986 cm^{-1} is the vibrational mode due to the out-of-plane deformation of *trans* CH=CH, shown in Figure 19b. This structure only appears in the polymer, thus is an accurate measure of the concentration of the polymer. Seen in Figure 21a, the decreasing concentration of the monomer is proportional to the disappearance of the absorbance band at 1591 cm^{-1}. The increasing concentration of the polymer can be determined by monitoring the appearance of the absorbance band at 986 cm^{-1} shown in Figure 21b. The plot of the monomer and polymer corrected absorbance vs. UV irradiation time is in displayed in Figure 22.

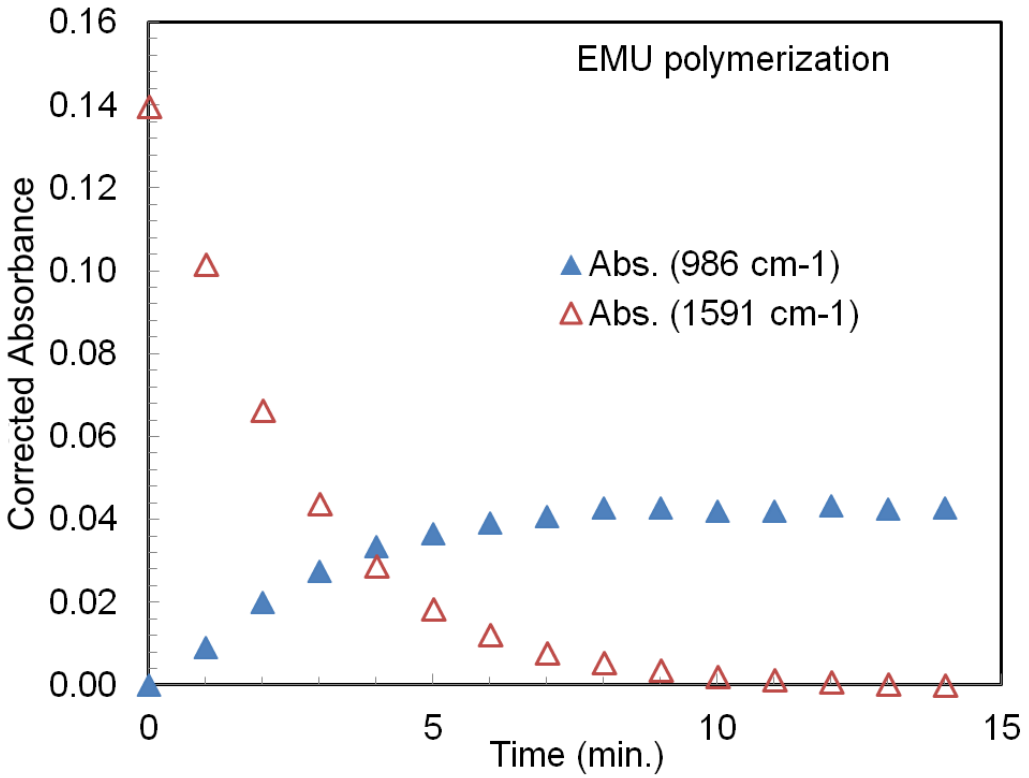

Figure 22. EMU monomer absorbance (1591 cm^{-1}) and poly-EMU absorbance (986 cm^{-1}) as a function of UV irradiation time. The polymerization was complete in an average of 14 minutes.

To determine the rate of polymerization, the absorbance of the monomer and polymer must be related to mole fraction. The mole fraction of polymer and monomer can be related to their absorbance using Lambert-Beer's law.

$$A_1 = \varepsilon_1 b X_1 \qquad (1)$$

$$A_2 = \varepsilon_2 b X_2 \qquad (2)$$

A is absorbance, ε is absorptivity, *b* is path length, and *X* is the mole fraction. (Calculating in terms of mole fraction is equivalent to concentration and more appropriate when in the solid state). Subscripts 1 and 2 refer to monomer, and polymer respectively. By definition, the mole fraction of monomer and the mole fraction of polymer sum to one, so equation 3 is derived from equations 1 and 2.

$$A_2 = -\frac{\varepsilon_2}{\varepsilon_1} A_1 + \varepsilon_2 b \qquad (3)$$

From the plot of A_1 vs. A_2 for both EMU and BMHA, shown in Figure 23,a least squares fit can be used to determine the slope which is equal to ($-\varepsilon_2/\varepsilon_1$) there by evaluating the absorptivities of the monomer and polymer. Solving equation 3 for path length, *b*, and replacing the equivalent variables for *b* in equation 1 gives equation 4 which is used to determine the mole fraction of monomer.

$$X_1 = \frac{1}{(A_2/A_1)(\varepsilon_1/\varepsilon_2)+1} \qquad (4)$$

It is important to note that the plot of A_1 vs. A_2 for both the polymerizations of BMHA and EMU are approximately linear which is a good indication that only the monomer and polymer are detected in the infrared spectrum at the analytical wavenumbers for this study, and not intermediate structures.

The term ($\varepsilon_1/\varepsilon_2$) is obtained by calculating the negative reciprocal of the slope of the plot of A_2 vs. A_1. The plot of Ln(X_1) vs. UV irradiation time, shown in Figure 24 yields a linear plot for both EMU and BMHA. This indicates the polymerizations of EMU and BMHA are approximately first order. Determining the line of best fit for the linear section of the kinetic curves gives a line with the slope equal to *k*, the pseudo first order rate constant for the polymerization.

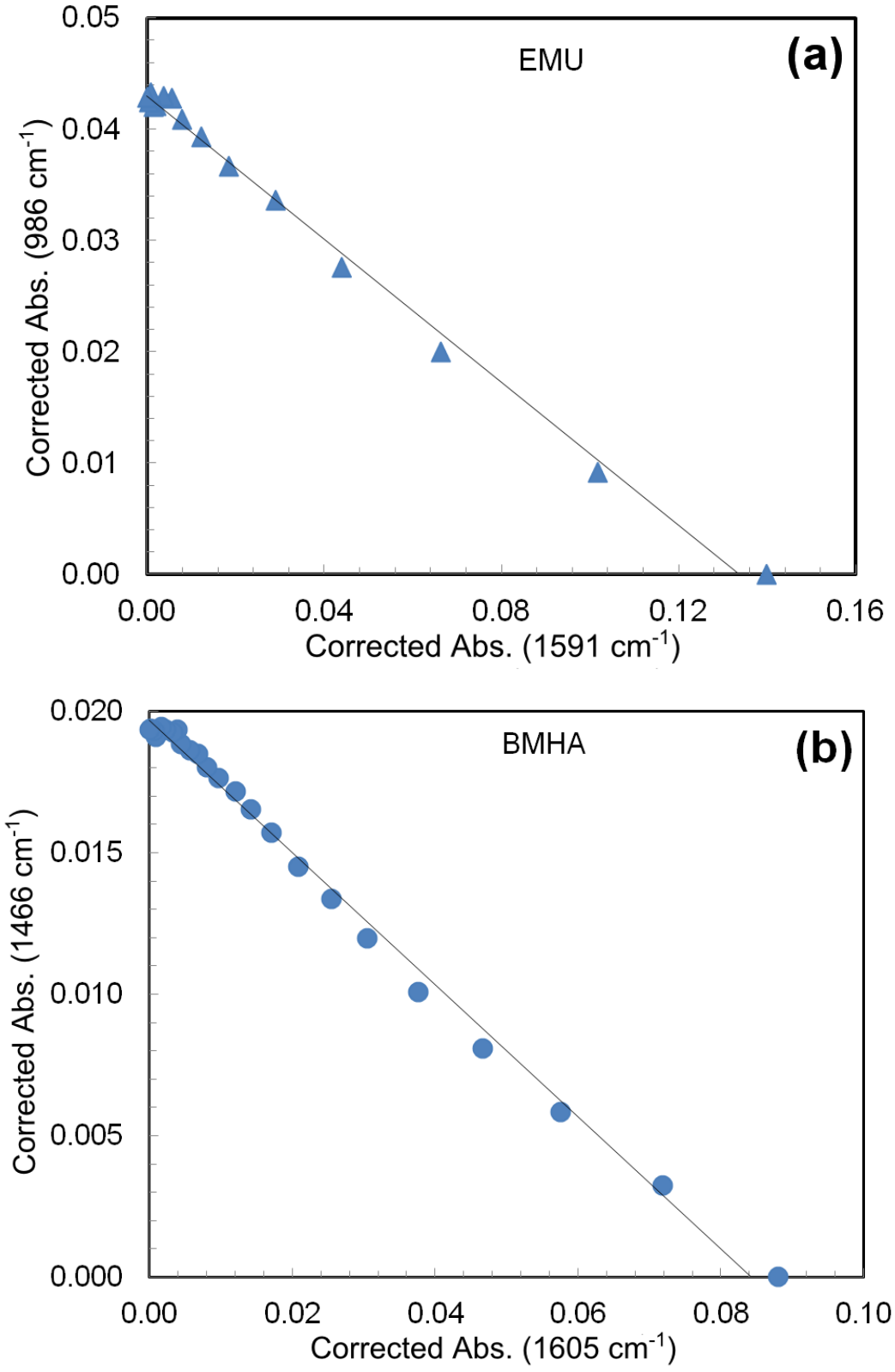

Figure 23. (a) Plot of corrected abs. 1591 vs. 986 cm^{-1} for EMU, and (b) plot of corrected abs. 1605 vs. 1466 cm^{-1} for BMHA. The slope of the trend line gives the value ($-\varepsilon_2/\varepsilon_1$).

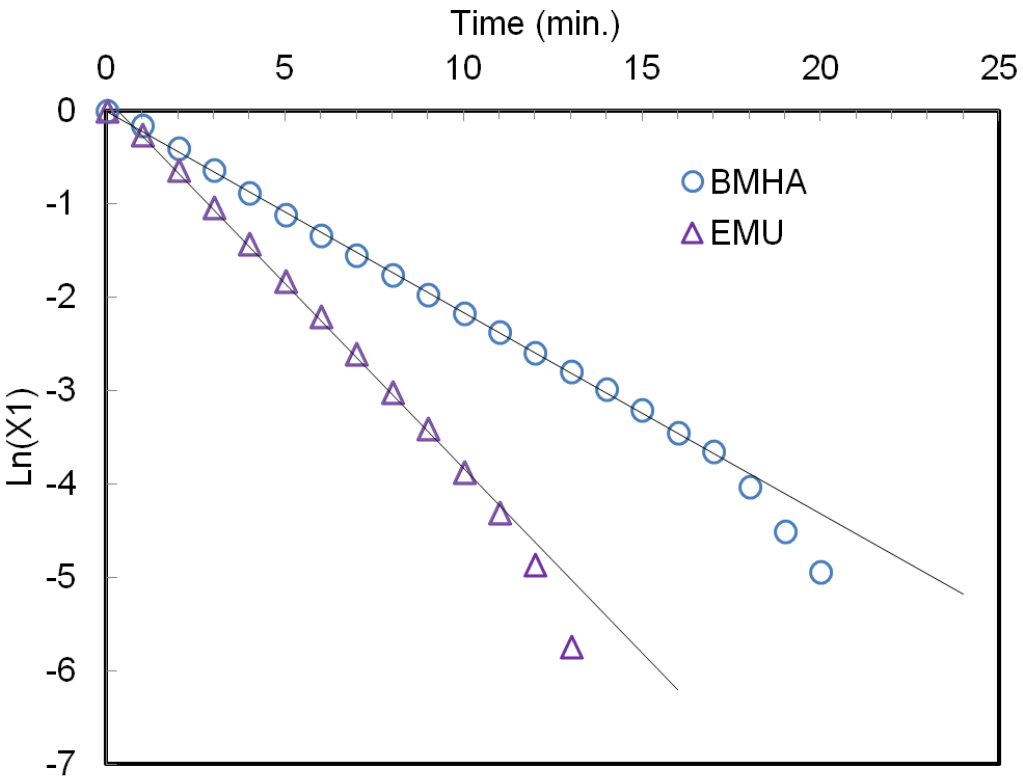

Figure 24. Plots of average Ln(X_1), vs. UV irradiation time for BMHA and EMU. The natural logarithms of monomer mole fraction are linear over the first five half lives of polymerization. (Error bars were smaller than data markers.)

The polymerization of EMU is reported to follow approximately the first order rate law which agrees with our results.[2] Because the polymerization of BMHA is similar to that of EMU, it is not surprising that BMHA also shows an approximately linear relationship between Ln(X_1) and UV irradiation time. That is to say, the polymerization of BMHA approximately follows pseudo first order reaction kinetics and its rate law may be written

$$rate = -\frac{dX_1}{dt} = kX_1$$

Or in the integrated form

$$\ln(X_1) = -kt$$

Where X_1 is the mole fraction of the monomer, and t is the UV light irradiation time. This stands to reason since the polymerization of BMHA is believed to be a radical chain initiation, unimolecular reaction of monomer to polymer. Since the reaction is not appreciably reversible, the reaction equation may be written

$$\text{Monomer} \xrightarrow{k} \text{Polymer}$$

where k is the rate constant. The kinetic curve reveals that the polymerization of BMHA is pseudo first order with respect to the concentration of the monomer.

Toward the end of the polymerization of BMHA and EMU, the rate of polymerization increases, shown in Figure 24. This behavior is seen in the literature for EMU.[2] We propose that the measured increase in rate is not systematic error, but a real increase in the rate of polymerization which happens when the crystal lattice is almost entirely polymer, making it easier, and therefore faster, for the remaining monomer molecules to form polymer and conform to the polymer crystal lattice.

Summarized in Table 4, results show that EMU (k = 0.394 min^{-1}) polymerizes more quickly than BMHA (k = 0.215 min^{-1}).

Table 4. Summary of rate constant data for BMHA and EMU.

Crystal	*Rate constant, k, ±std. dev. (min^{-1})*	*Half life (min.)*
BMHA	0.215 ±0.016	3.22
EMU	0.394 ±0.036	1.75

This kinetic experiment is limited in that it provides a relative rate constant, not an absolute one. Because the rate of polymerization is dependent upon the number of photons absorbed by the monomer and the absolute number of photons is not standardized, this kinetics method is relative. It is useful for making comparisons between polymerizations conducted using this method because the light source and its

intensity incident to the sample disc did not change between measurements of EMU and BMHA.

2.4 Further Kinetic Method Development

For this method of kinetics determination to be useful for future research, the entire method of obtaining kinetics data must be reproducible, not just the measurement. The average rate constants and uncertainties reported in Table 4 are a reflection of the reproducibility of only a part of the entire method: KBr disc preparation and the sample measurement. Further, these rate constants were determined by a single operator in only one laboratory.

The entire experimental method involves synthesis, purification, and recrystallization of the monomer in addition to sample storage, sample preparation, the kinetic measurement, and data processing. We predict that of these steps, the sample preparation and the kinetic measurement will introduce a majority of the error. Monomer synthesis, recrystallization, storage, and data processing are facile steps in the method. Monomer synthesis and recrystallization are well defined in the literature and easy to reproduce in the laboratory. Data processing requires no estimation or interpretation by the operator so error from processing is small. Making these assumptions, the error of the entire method can be approximated by the error reported for only the sample preparation and kinetic measurement; however these assumptions have yet to be substantiated.

After the average rate constant for BMHA was determined, a new sample of BMHA in KBr was created with the same mole fraction as the previous test sample (0.00139 mol/mol, 0.199% w/w) and the rate constant, *k*, of 0.228 min^{-1} was determined.

This value is statistically indistinguishable from the average rate constant found for the polymerization of BMHA because is falls within three standard deviations of the measured mean. In fact, the new value was within one standard deviation of the measured mean. This result shows the sample preparation and measurement are reproducible in the hands of a single operator. Determining the error of the entire measurement in the hands of different operators and operators with less experience is as yet understood.

2.5 Kinetic Method Error Discussion

As mentioned previously, we predict that most of the error in the method arises from the sample preparation and the kinetic measurement. Many factors affect the rate of polymerization and every reasonable effort was made to control them. Sample temperature, the concentration of crystal irradiated, UV light wavelength and power, and KBr disc quality are all variables which have an effect on polymerization rate. The following is a discussion of the possible sources of error and future method improvements which may be tested for their ability to reduce error.

Sample Temperature

Temperature is certainly a factor in solid state photochemical kinetics. Increasing temperature speeds reaction rates in solution. The effect of temperature on topochemical reactions can either increase or decrease the reaction rate. For the polymerization of EMU, crystal temperature has a significant effect on reaction rate.[15] Polymerization only proceeds between -20-50 °C. Below -20 °C, the monomer does not form polymer and above 50 °C, the monomer crystal melts (mp. 53-54 °C). In the range -20-50 °C, the rate of polymerization increases as temperature increases. The dimerization of 2-Benzyl-5-

benzylidenecyclopentanone, reported by Honda,[16] showed first order kinetics over a wide temperature range with a maximum rate at 200K. The rate decreased at temperatures above ~250K and below ~173K. The temperature dependence of the reaction's kinetics was attributed to the changes in the crystal lattice rigidity.

Because temperature has been shown to affect the rate of solid state reactions, temperature was kept constant during all kinetic measurements, despite the inability to control sample temperature. The temperature inside the transmission space was monitored, and it was assumed that the sample was in thermal equilibrium with the nitrogen atmosphere inside the transmission space. Before infrared spectra were collected, the sample KBr disc containing monomer crystal was given time (~15 min.) to equilibrate with the surrounding atmosphere.

Temperature remained steady during the repeated polymerization trials and varied little between the measurements of BMHA and EMU polymerizations. For every trial of BMHA and EMU polymerization, the temperature during one kinetic measurement did not change by more than 0.2 °C, and for a majority of the trials, the temperature did not change within the temperature measurement resolution. Over five trials of EMU polymerization, the temperature ranged from 27.3-28.3 °C with an average across the five trials of 28.0 °C (301.1 K). Over five trials of BMHA polymerization, the temperature ranged from 29.0-29.5 °C with an average of 29.3 °C (302.4 K). The average temperature difference between measurements of EMU and BMHA was 1.3 K, or 0.4% of the mean temperature, in Kelvin, across all trials. Measured rate constants were plotted against temperature and no significant relationship was found between

temperature and rate constant for either BMHA or EMU, suggesting that the error due to temperature variance was a small contribution to total error.

Concentration of Monomer Irradiated in KBr

A surprising finding during method development was that the amount of monomer crystal irradiated in the KBr disc, or the concentration of monomer crystal in KBr, had an effect on the rate of polymerization. After many trials of the kinetic measurement, a plot of BMHA monomer absorbance at 1605 cm^{-1} vs. rate constant, *k*, shown in Figure 25 indicated a clear trend that the rate of reaction increased with decreasing amount of monomer irradiated.

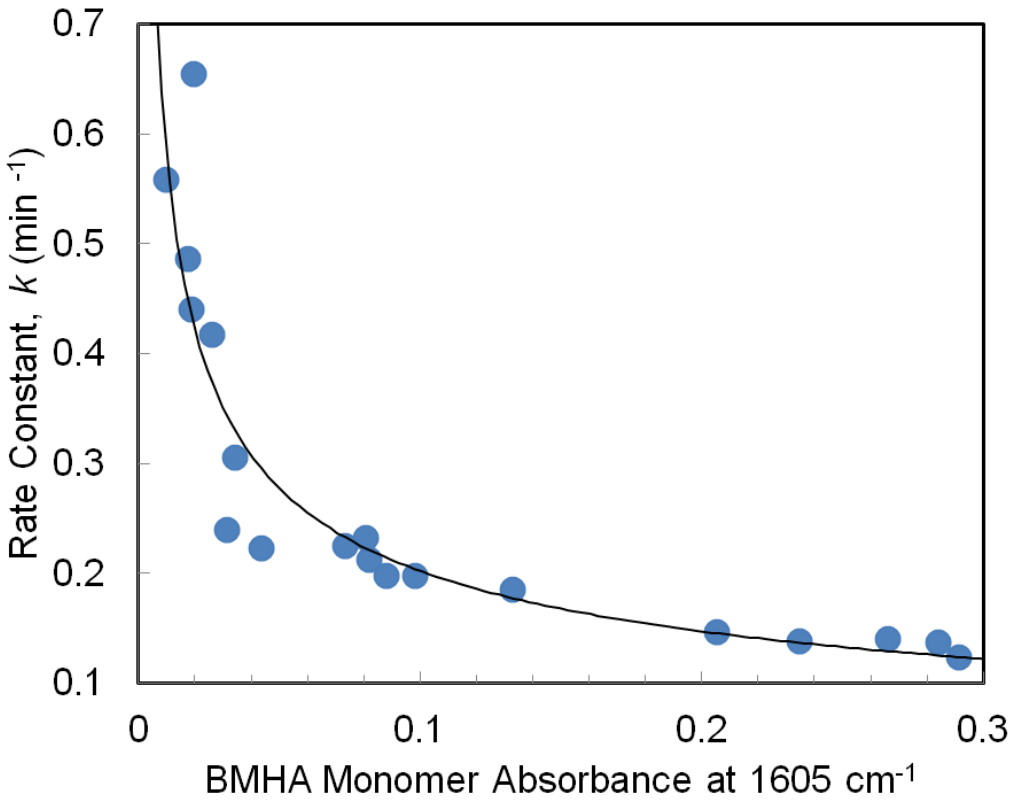

Figure 25. The rate constant, *k*, plotted against BMHA monomer's absorbance at 1605 cm^{-1}, proportional to the amount of the crystal irradiated, shows the polymerization rate increased when less monomer was irradiated in KBr.

A rationale for this behavior has not been fully developed, but this trend may exist if the photons from the UV source are not in great excess to the monomer crystal, causing the effective concentration of photons to increase as the initial mass of monomer crystal is decreased in the KBr disc.

Absorbance was used as a measure of the amount of monomer in KBr because, according to the Lambert-Beer law, absorbance is proportional to the concentration of sample in KBr and to the path length of the disc. A power function best fits the relationship between monomer absorbance and rate constant. The reason for this trend is not understood and remains for future exploration. The concentration of monomer in KBr was reduced further in hopes of discovering a concentration below which the reaction rate did not change, but none was found. As the concentration of monomer in KBr was reduced, the signal to noise ratio became unacceptable before a maximum rate of polymerization was reached. This obstacle led to the need to produce samples of monomer crystal in KBr of equal mole fraction in order to compare rate constants of different polymerizations. As a result, the rate constants reported are relative to this system of measurement. In the future, determining the factor which causes rate to change with the amount of monomer irradiated is a future task which will allow for the measurement absolute rate constants.

Power of the UV Source

The power of the pulsed xenon source irradiating the KBr sample disc was 32.6±0.1 μW (± 1 Standard Deviation) and was shown to drift ±0.1 μW during a 30 minute period.

Power of the light irradiating the sample disc was evaluated by measuring the power of the light that passed through a blank KBr sample washer in the UV irradiation apparatus set up in the FT-IR spectrometer. The light collection probe was placed as close to the sample washer as possible without contact between the two. The UV source was powered on for 30 minutes to measure the average power emitted as well as the drift in the power of the pulsed xenon source. This measurement was repeated three times to obtain an average value for light source power. Before each repeated measurement, the light collection probe was removed and reset to ensure reproducibility of this measurement in the future.

The average power irradiating the KBr sample disc was 32.6±0.1 μW. Drift in the power of the UV source over time was quite small amounting to ±0.1 μW above and below the average power for each measurement. The 30 minute window over which drift was measured is slightly longer than the time required to complete one kinetic measurement for BMHA. Therefore, we can assume the power of the UV source does not change significantly during the course of the kinetic measurement. The source also emitted the same power over three 30 minute windows so we can assume that across multiple trials of the kinetic measurement, the crystal sample received the same light intensity from the lamp. Based on these results, error from change in the power of the pulsed xenon light source was estimated to be a small contributing factor to total measurement error.

Quality of the KBr Disc

Much of the method error may arise from the inconsistencies between sample KBr discs used for the infrared kinetic measurement. This is because KBr is the medium

through which UV light must penetrate in order to reach the crystal monomer to initiate polymerization. Variations in the KBr disc lead to inconsistencies in the UV light transmission as well as non-standard path lengths leading to inconsistent sample irradiation in different KBr discs.

The clarity of the KBr disc affects light transmission of both UV and infrared radiation. Sample discs with lower light transmission would allow lower penetration of UV light, reducing the number of photons incident to the monomer crystal. This changes the effective concentration of photons which will have an effect on the rate because photons are considered a reactant in photochemical polymerizations. The hand held die press consistently produced discs which were suitable for measurement, but often contained cracks or clouds, reducing transmission. With this device, strict control of these KBr disc flaws was not possible.

Another concern of inconsistent KBr discs was the inability to control path length among kinetic measurements. While care was taken to place the same mass of KBr/sample solution in the die press and apply the same pressure to the die for each repetition of the measurement, the hand held die press was not able to produce discs of consistent path length. The design of the hand held die press allowed the KBr to spread out of the sample washer as the disc was pressed so that path length was not controlled by the amount of material added to the die. Altering the disc path length varies the distance of the monomer to the UV source. In addition, the penetration of the UV light may be reduced as its depth in the KBr disc increases, reducing the photons received by monomer contained in the portion of the disc furthest from the UV source. The effects of path length and sample disc transmission on polymerization rate have not been

determined, but these variables should be investigated for increasing the method's precision.

To reduce error in the method resulting from KBr disc inconsistencies, a more reliable method of producing high quality KBr discs may be needed. Evacuable KBr dies provide the best reproducibility and are required by some ASTM standard methods because they generate consistent discs.[17] Employing an evacuable die may help reduce error associated with inconsistencies in the KBr sample disc.

CHAPTER THREE: CONCLUSIONS

Our results show that we have been successful in creating a method for studying the kinetics of topochemical reactions and in applying that method to determine the rate laws and relative rate constants for the 1,4-polymerizations of BMHA and EMU. The method is standard for our laboratory, but more testing will need to be done to ensure reproducibility in the hands of future operators.

We have also demonstrated the heterogeneous nature of the topochemical polymerization of BMHA through X-ray powder diffraction measurement, owing to the discovery that BMHA polymerizes by X-ray irradiation.

Furthermore, differential thermal analysis revealed that the polymerization of BMHA is initiated by heating. Differential thermal analysis also gave the enthalpy of polymerization and allowed a crude calculation of the lattice strain energy of the reaction.

In the future, we hope to provide additional information on the polymerization of BMHA, such as activation energy, E_a. This can be accomplished by measuring the rate constant over a range of temperatures and using the Arrhenius equation to calculate the energy of activation. To further develop the kinetic method reported in this paper, it will be necessary to investigate the cause for the increased reaction rate with decreasing concentration of monomer irradiated in the KBr disc. Addressing this unexpected result will help to standardize the kinetic method for future research.

CHAPTER FOUR: EXPERIMENTAL SECTION

4.1 General Methods

NMR and IR spectra were recorded on a Joel Eclipse 300 FT-NMR and Nicolet Avatar 370 DTGS FT-IR spectrometer, respectively. A Rigaku Miniflex powder diffractometer was used to record X-ray powder diffraction profiles. Differential thermal data was recorded on a Perkin-Elmer Pyris Diamond thermogravimetric/differential thermal analyzer.

4.2 X-ray Powder Diffraction

Measurements were recorded at room temperature using a Rigaku Miniflex diffractometer with a Cu-Kα line. The X-Ray generator was set at a power of 30kV and 15mA. Milled BMHA crystals were affixed to a glass slide with a thin layer of silicone grease. The crystals were spread over the grease leaving a smooth surface. It was discovered that polymerization proceeded under X-ray irradiation, so diffraction profiles were measured continuously until polymerization was complete. Measurement parameters: 2°/minute scan speed, 0.02° step width, 10-40° 2θ sweep. Infrared analysis to confirm the polymer synthesis by X-ray irradiation was performed on a Smiths IdenifyIR FT-IR spectrometer with the ATR sampling accessory.

4.3 Differential Thermal Analysis

Differential thermal analysis was completed on a Perkin-Elmer Pyris Diamond TG/DTA with 200 mL/minute nitrogen purge. The temperature was set to ramp from 50-140 °C at a rate of 5 °C/minute, followed by a slower ramp from 140-200 °C at 1 °C/minute. After reaching the maximum temperature, the sample was cooled to 50 °C.

Infrared analysis of the heat induced polymer was conducted on a Perkin Elmer Spectrum One FT-IR using the ATR sampling accessory.

4.4 Kinetic Measurement by FT-IR Spectroscopy

Instrumentation

In order to measure the infrared absorbance spectrum of BMHA and EMU over the course of polymerization, a Nicolet Avatar 370 DTGS FT-IR spectrometer was modified to allow UV irradiation and transmission FT-IR measurements of the sample without disturbing its position. The transmission accessory for the spectrometer was purged under nitrogen atmosphere for the duration of the measurement. Ultraviolet light from an Ocean Optics PX-2 pulsed xenon light source was directed into the transmission chamber via an Ocean Optics P600-1-SR UV-visible transparent fiber. The pulsed xenon source was controlled by a 3M Powerface controller set at a rate of 100 pulses per second. The fiber was aimed at the KBr disk from an angle so as not to obstruct the infrared beam path. The power of the light irradiating the sample was 32.6±0.1 μW measured with a Thor Labs PM100D power meter with the 50mW light collecting accessory (P.N. S130VC). The sample temperature was recorded with a Vernier LabPro digital temperature probe mounted inside the transmission space. The UV irradiation assembly in the FT-IR spectrometer can be seen in Figures 25 and 26.

Figure 26. View of the UV irradiation apparatus inside the transmission space of the infrared spectrometer. The UV fiber is held in the three-prong clamp and the temperature probe is mounted below it.

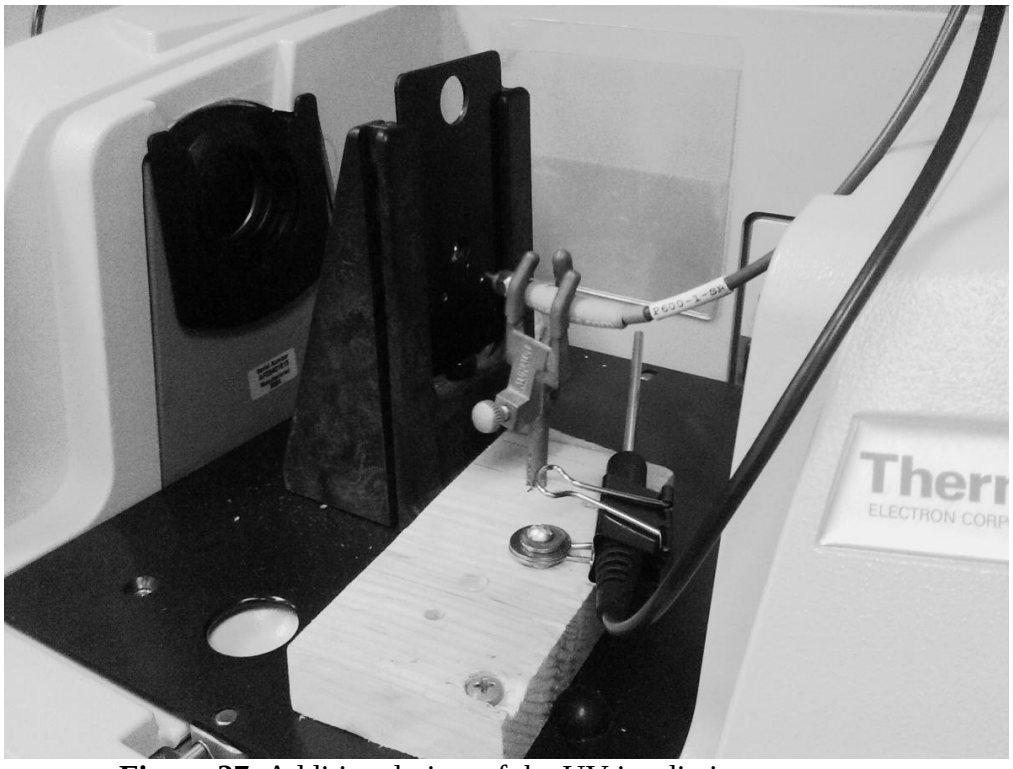

Figure 27. Additional view of the UV irradiation apparatus.

Sample Preparation

Potassium Bromide sample transmission discs for infrared analysis were pressed with a Pike Technologies 3mm KBr die (P.N. 161-1024) in combination with a Perkin-Elmer hand held die press using Fisher Scientific IR grade KBr (P. 227) which was dried in an oven at 140°C overnight before use and store in a dessicator. Both BMHA and EMU samples were milled into a fine powder in a miniature ceramic mortar/pestle. Because of the difficulty of producing a high quality, high transmission disc when using pulverized salt, the KBr was not milled into a powder, but used directly from the bottle without further milling.

It was determined that the amount of BMHA crystalline monomer irradiated in the KBr disc had an effect on the rate constant of the reaction, so it was necessary to create KBr solutions of BMHA and EMU with the same mole fraction. A target of 0.2% w/w of BMHA in KBr was selected because it kept the concentration of sample low so that Lambert-Beer's law could be assumed, it gave a rapid polymerization, and it provided sufficient absorbance values of analytical peaks. A sample of 0.202% BMHA in KBr was prepared by first creating a 2.02% stock solution by weighing 10.1 mg of powder BMHA and increasing the total mass to 500.0 mg with KBr. The BMHA solution was mixed by shaking (without milling ball) in a Wig-l-bug amalgamator for 30 seconds.

$$\frac{10.1\ mg\ BMHA}{500.0\ mg\ total\ mass} = 2.02\%\ w/w$$

From the stock solution, 99.9 mg were weighed and the total mass was increased to 1000.0 mg with KBr to yield a BMHA solution of 0.202% w/w. This solution was also mixed by 30 seconds of shaking (without milling ball) in an amalgamator.

$$\frac{(2.02\%\ w/w) \cdot (99.9\ mg\ stock\ BMHA)}{1000.0\ mg\ total\ dilute\ mass} = 0.202\%\ w/w\ BMHA$$

The mole fraction of BMHA in the 0.202% mass fraction was determined to be 0.00141 mol/mol by converting the mass of each component to moles.

$$0.202\%\ w/w\ BMHA = \frac{0.202\ mg\ BMHA}{99.798\ mg\ KBr + 0.202\ mg\ BMHA}$$

$$= \frac{0.00118\ mol\ BMHA}{0.838\ mol\ KBr + \ 0.00118\ mol\ BMHA}$$

$$= 0.00141\ mol\ fraction\ BMHA$$

The solution of EMU in KBr with the same mole fraction has the same mole values presented in the above equation, but has a different mass percent because EMU has a greater molecular weight that BMHA (198.217 g/mol compared to 170.163 g/mol, respectively). When the mole values which give a 0.00141 mol/mol EMU solution are converted to mass, the solution of EMU with the same mole fraction as the 0.202% w/w BMHA solution has a 0.234% w/w concentration.

$$\frac{0.00118\ mol\ EMU}{0.838\ mol\ KBr + 0.00118\ mol\ EMU} = \frac{0.233\ mg\ EMU}{99.798\ mg\ KBr + 0.233\ mg\ EMU}$$

$$= 0.234\%\ w/w\ EMU$$

Thus the target concentration for the EMU solution was 0.234% w/w EMU in KBr. A 0.235% w/w solution of EMU for IR analysis was created in the same manner described for the BMHA solution.

When preparing to press the KBr discs, the die set was wiped with a lint-free wipe without using water or acetone to clean the die surfaces. Introducing any water, even the miniscule amount in acetone, caused the KBr disc to stick to the die faces and fracture when removed from the die. To store the KBr die set, the dies were rinsed with distilled

water to remove KBr, which is highly corrosive to metals, dried with a lint-free wipe, and housed in a desiccator.

Because the concentration of monomer crystal irradiated in KBr was shown to have an effect on the polymerization rate, the path length of each disc had to be controlled in addition to the solution concentration. For each disc, 50 mg of KBr/sample solution were added to the lower well of the die, and uniform pressure was applied to each disc by setting in place the pressure dial for the hand press.

Data Collection

FT-IR measurements of the polymerization process were collected at a resolution of 2 wavenumbers (cm^{-1}) with 8 scans averaged per spectrum. The sample KBr disc was irradiated for 1 minute intervals until the polymerization process completed. Measurements were carried out at room temperature without the capacity for temperature control. Temperature inside the transmission chamber ranged from 29.0-29.5°C over the course of five trials of the BMHA polymerization with the temperature profile during any one trial not changing more than ±0.1°C. During five trials of EMU polymerization temperature ranged from 27.3-28.3°C with the temperature during any one trial not changing more than ±0.2°C.

4.5 Synthesis

***(Z,Z)*-2,4-hexadienedioate (EMU)[8,12]**

(Z,Z)-muconic acid (1.42g, 9.99mmol), thionyl chloride (1.49mL, 20.56mmol), and dimethylformamide (1 drop) were added to a 100-mL round bottom flask with dry dichloromethane (50mL) under inert argon atmosphere. The solution was refluxed with stirring for five hours. The solution appeared brown and cloudy with some solid white

material remaining. After reflux, the solution was cooled to room temperature with continued stirring. The reaction solution was added drop wise via canula to a stirring solution of ethanol (12.87mL, 199.8mmol) and triethyl amine (1.5mL, 10.76mmol) dissolved in dry dichloromethane (50mL) at 0 °C. A white gas appeared over the muconic ester solution as muconic acid chloride was dripped in. The reaction mixture was allowed to stir for one day as it warmed to room temperature. The solution appeared clear yellow orange. The solution was washed once with 0.1 molar HCl, once with de-ionized water, and once with saturated sodium chloride solution. The organic layer was removed and dried over anhydrous magnesium sulfate. The solvent was evaporated and the muconic ester was further purified by silica gel chromatography with 1,2-dichloroethane as the elution solvent. The fractions containing EMU were combined and the solvent was evaporated. EMU was recrystallized from hexanes by slow solvent evaporation. Clear, needle-like crystals resulted. Yield 0.328 g (18.6%). $R_f = 0.30$. ^{1}H-NMR 300 MHz ($CDCl_3$): δ 7.38 (dd, 2H), δ 5.96 (dd, 2H), δ 4.19 (q, 4H), δ 1.30 (t, 6H). ^{13}C-NMR 300MHz ($CDCl_3$): δ 166.05, 128.19, 124.59, 60.77, 14.55. FT-IR (KBr disc): 3405.7, 3086.4, 2986.0, 2905.0, 1715.1, 1591.6, 1478.5, 1455.8, 1369.9, 1351.1, 1229.3, 1216.3, 1170.7, 1031.7, 941.9, 878.2, 833.2, 809.0, 751.7, 667.8, 418.6 cm^{-1}.

Diethyl 3,4-bis(methylene)hexanedioate[3,18]

Dry, distilled triethyl orthoacetate (52.08mL, 284.14mmol), 2-butyne-1,4-diol (4.438g, 51.42mmol), and propionic acid (0.521mL, 6.956mmol) were added to dry dimethyl formamide (50mL) under inert argon atmosphere with stirring. The reaction solution was refluxed for 8 minutes, open to atmosphere, in a modified Sunbeam household microwave oven (2450 MHz, 120V) on high power. The solution appeared

clear orange. The solution was diluted with ethyl acetate, washed three times with 0.5 molar HCl, three times with saturated sodium chloride solution, then the ethyl acetate layer was dried over magnesium sulfate, filtered, and the solvent was evaporated. The resulting diethyl ester compound was used for the systhesis of 3,4-bis(methylene)hexanedioic acid without further purification.

3,4-bis(methylene)hexanedioic acid (BMHA)

Diethyl-3,4-bis(methylene)hexanedioate (1.52g, 6.70mmol) was added to 1.0 molar sodium hydroxide solution (14.7mL, 14.7mmol) in ethanol (20mL). The clear orange solution was placed in a room temperature water bath and stirred for two hours. The reaction solution was then chilled to 0 °C in an ice bath, diluted with de-ionized water (10mL) and then the pH adjusted to 3 by adding concentrated HCl. After adjusting the pH, the solution appeared yellow. The reaction mixture was extracted five times with ethyl acetate and the resulting solution was dried over anhydrous magnesium sulfate. The solution was filtered and the solvent evaporated. The resulting precipitate was rinsed with cold ethyl acetate. Yield 0.76g (10.3%). ^{1}H-NMR 300 MHz (DMSO-D_6): δ 12.22 (s, 2H), δ 5.22 (s, 2H), δ 5.12 (s, 2H), δ 3.20 (s, 4H). ^{13}C-NMR 300 MHz (DMSO-D_6): δ 172.9, 140.5, 117.0, 40.0. FT-IR (KBr disc): 3092.5, 3020.1, 2924.0, 2728.6, 2626.6, 2544.5, 2361.9, 2339.9, 1697.2, 1603.6, 1419.2, 1325.7, 1289.9, 1231.4, 1141.9, 964.4, 944.5, 919.7, 901.6, 732.6, 667.8, 644.8, 591.6, 503.5, 423.7, 417.1 cm^{-1}.

REFERENCES

[1] Turowska-Tyrk, I. Structural transformations in organic crystals during photochemical reactions. *J. Phys. Org. Chem.* **2004**, 17, 837-847.

[2] Tashiro, K. Structural change in the Topochemical Solid-State Polymerization Process of Diethyl cis,cis-Muconate Crystal. 1. Investigation of Polymerization Process by Means of X-ray Diffraction, Infrared/Raman Spectra, and DSC. *Macromolecules.* **1999**, *32*, 2449-2454.

[3] Beard, K. Crystal Engineering: Solid State Reactivity of Butadiene Monomers in Crystals. M.S. Thesis, Western Carolina University, December 2008.

[4] Tieke, B. Polymerization of Butadiene and Butadiyne (Diacetylene) Derivatives in Layer Structures. *Adv. Polym. Sci.* **1985,** *71,* 79.

[5] Schmidt G.M.J., Cohen M.D. Topochemistry. Part I. A Survey. *J. Chem. Soc.* **1964,** 1996-2000.

[6] Kearsley, S.K. The Prediction of Chemical Reactivity Within Organic Crystals Using Geometric Criteria. In *Organic Solid State Chemistry*; Desiraju G.R., Eds.; Studies in Organic Chemistry Series; Elsevier: Amsterdam, The Netherlands, 1987; pp 69-115.

[7] Matsumoto, A. Stereocontrol of Diene Polymers by Topochemical Polymerization of Substituted Benzyl Muconates and Their Crystallization Properties. *J. Polymer Science; PartA: Polymer Chemistry*. **2006,** 4952-4965.

[8] Matsumoto, A. Stereospecific Polymerization of Dialkyl Muconates through Free Radical Polymerization: Isotropic Polymerization and Topochemical Polymerization. *Macromolecules.* **1996,** *29*, 423-432.

[9] Nagahama, S. Two-Dimensional Hydrogen Bond Networks Supported by CH/π Interaction Leading to a Molecular Packing Appropriate for Topochemical Polymerization of 1,3-Diene Monomers. *Crystal Growth & Design*, **2003,** *3*, 247-256.

[10] Harvey, David. Kinetic Methods. *Analytical Chemistry 2.0*, Open Source, Creative Commons.

[11] Wegner, G. Solid-State Polymerization Mechanisms. *Pure & Appl. Chem.* **1977,** *49*, 443-454.

[12] Matsumoto, A. Crystal Engineering for Topochemical Polymerization of Muconic Esters Using Halogen-Halogen and CH/π Interactions as Weak Intermolecular Interactions. *J. Am. Chem. Soc.* **2002,** *124*, 8891-8902.

[13] Rodriquez, F. Polymerization Processes. *Principles of Polymer System*, 2nd edition; McGraw-Hill Chemical Engineering Series; Hemisphere Publishing: Washington, 1982; pp 106.

[14] Billmeyer Jr. F. Radical Chain (Addition) Polymerization. *Textbook of Polymer Science*, 2nd edition; Wiley-Interscience: New York, 1971; pp 306, 307.

[15] Matsumoto, A. Crystalline-State Polymerization of Diethyl *(Z,Z)*-2,4-Hexadienedioate via a Radical Chain Reaction Mechanism to Yield an Ultrahigh-Molecular-Weight and Stereoregular Polymer. *Macromolecules.* **1998**, *31*, 2129-2136.

[16] Honda, K. Kinetic and Mechanistic Study on Single-Crystal-to-Single-Crystal Photodimerization of 2-Benzyl-5-benzylidenecyclopentanone Utilizing X-ray Diffraction. *J. Am. Chem. Soc.* **1999,** *121,* 8246-8250.

[17] Specac: IR Sampling Accessories & Press Solutions. http://www.specac.com/products/pellet-press-dies/evacuable-pellet-dies/509 (accessed Feb 24, 2012).

[18] Srikrishna, A. Application of Microwave Heating Technique for Rapid Synthesis of γ,δ-Unsaturated Esters. *Tetrahedron.***1995,** *51*,1809-1816.